

Quantum delocalization on correlation landscape: The key to exponentially fast multipartite entanglement generation

Yaoming Chu,¹ Xiangbei Li,¹ and Jianming Cai^{1,*}

*¹School of Physics, Hubei Key Laboratory of Gravitation and Quantum Physics,
International Joint Laboratory on Quantum Sensing and Quantum Metrology,
Institute for Quantum Science and Engineering,
Huazhong University of Science and Technology, Wuhan 430074, China*

Abstract

Entanglement, a hallmark of quantum mechanics, is a vital resource for quantum technologies. Generating highly entangled multipartite states is a key goal in current quantum experiments. We unveil a novel framework for understanding entanglement generation dynamics in Hamiltonian systems by quantum delocalization of an effective operator wavefunction on a correlation landscape. Our framework establishes a profound connection between the exponentially fast generation of multipartite entanglement, witnessed by the quantum Fisher information, and the linearly increasing asymptotics of hopping amplitudes governing the delocalization dynamics in Krylov space. We illustrate this connection using the paradigmatic Lipkin-Meshkov-Glick model and highlight potential signatures in chaotic Feingold-Peres tops. Our results provide a transformative tool for understanding and harnessing rapid entanglement production in complex quantum systems, providing a pathway for quantum enhanced technologies by large-scale entanglement.

* jianmingcai@hust.edu.cn

Introduction

Entanglement, a distinctive property that sets the quantum realm apart from its classical counterpart, is a vital resource for the development of quantum technologies. One of the most paramount objectives in modern quantum experiments is the rapid generation of multipartite entanglement from readily available non-entangled states, particularly at an exponentially fast speed [1, 2]. This is crucial for two primary reasons. Firstly, multipartite entanglement is essential for unveiling foundational problems in quantum mechanics, such as the puzzling quantum-to-classical boundary [3], quantum nonlocality [4], and a wide range of quantum many-body effects [5]. The exponentially fast generation of multipartite entanglement with an ultra-short evolution time, which could enhance robustness against decoherence [6], is of particular interest for exploring the fundamental question: what is the maximum achievable macroscopic entanglement in realistic quantum systems [7]? Secondly, multipartite entanglement holds immense potential as a critical resource for revolutionizing modern information technologies. Harnessing large-scale entangled states underscores the power of groundbreaking advances over classical counterparts in the latest developments of quantum-enhanced precision measurement [8–12], high-speed computation [13–15], and secure communication [16–18]. The speed of entanglement generation is crucial for improving the duty ratio of quantum information processing tasks and sustaining quantum advantages [19, 20], with approaching the elusive Heisenberg limit in quantum metrology [21] as a notable example.

Unfortunately, not only the generation of entangled state but also the analysis of entangling dynamics in large-scale quantum experiments face unprecedented complexity and remain challenges. While the celebrated Lieb-Robinson bounds suggest the tantalizing possibility of exponentially fast entanglement generation with long-range interactions [22, 23], they fall short of pinpointing explicit interacting many-body systems that can realize this ambitious objective. To tackle this pivotal problem, we propose an approach that synergistically integrates two foundational concepts in quantum information theory and quantum physics: quantum Fisher information (QFI) [24, 25] as a potent witness of multipartite entanglement [26–30], and quantum delocalization that is a captivating phenomenon underpinning a plethora of cutting-edge quantum effects such as thermalization, scrambling, and hydrodynamics in many-body systems [31–35]. By harnessing the power of QFI and quantum delocalization in tandem, we aim to elucidate the intricate dynamics of entanglement generation in complex quantum systems and identify specific systems that can achieve exponentially fast generation of multipartite entanglement.

In this work, we demonstrate that the intricate dynamics of QFI can be elegantly captured by

delocalizing an effective 2D wavefunction on a meticulously crafted correlation landscape, defined within an efficient operator subspace. By exploiting the Krylov approach [36] to construct this subspace, we establish a comprehensive paradigm for accessing the exponentially fast generation of multipartite entanglement. Our analysis uncovers an intriguing link between the exponentially fast entanglement generation and the linear increase of Lanczos coefficients in Krylov space, thereby providing a deeper understanding of the mechanisms driving rapid entanglement creation. We illustrate the power and versatility of our approach using the paradigmatic Lipkin-Meshkov-Glick model [37] and extend our analysis to generic chaotic dynamics, highlighting the broad applicability of our results in the context of exponentially fast entanglement production.

General framework for characterizing QFI evolution in many-body systems

The quantum Fisher information (QFI) sets the ultimate limit for measurement precision in quantum metrology [24], quantifying the sensitivity of a quantum state ρ to a unitary transformation generated by a Hermitian interrogation operator \hat{O} associated with a parameter ϑ to be estimated. The attainable parameter estimation uncertainty is constrained by the quantum Cramér-Rao bound, $(\Delta\vartheta)^2 \geq 1/F_Q[\rho, \hat{O}]$, where $F_Q[\rho, \hat{O}]$ represents the QFI of the parametrized quantum state $\rho_\vartheta = e^{-i\vartheta\hat{O}}\rho e^{i\vartheta\hat{O}}$. To enhance sensing performance in a metrological task, an entangled input state ρ exhibiting large QFI for $N > 1$ particles is sought. Remarkably, the entanglement depth \mathcal{E}_d of a multipartite quantum state [namely the state is \mathcal{E}_d -producible, but not $(\mathcal{E}_d - 1)$ -producible] is delicately linked to the QFI density through $\mathcal{E}_d \geq F_Q/N$ [28] for the standard scenario of a local $\hat{O} = \sum_{i=1}^N \hat{o}_i$. Consequently, achieving the Heisenberg limit ($F_Q \simeq N^2$) necessitates preparing a globally entangled state with $\mathcal{E}_d \sim N$.

Here, we consider the preparation of an entangled state from a readily accessible product state σ through unitary evolution governed by the Hamiltonian \mathcal{H} . The QFI of $\rho(t) = e^{-i\mathcal{H}t}\sigma e^{i\mathcal{H}t}$, associated with the interrogation operator \hat{O} , can be formulated in the following form [21],

$$F_Q[\rho(t), \hat{O}] = 2\gamma \text{tr}([\hat{O}(t), \sqrt{\sigma}]^\dagger [\hat{O}(t), \sqrt{\sigma}]), \quad (1)$$

where $\gamma \in [1, 2]$, and $\hat{O}(t) = e^{i\mathcal{H}t}\hat{O}e^{-i\mathcal{H}t}$. This formula relates the QFI dynamics during the state preparation to the evolution of the interrogation operator in Heisenberg picture. Exploiting the Liouvillian superoperator, the time-evolved interrogation operator can be expressed as

$$\mathcal{L} = [\mathcal{H}, \bullet], \quad \hat{O}(t) = e^{i\mathcal{L}t}\hat{O} = \sum_{n=0}^{\infty} \frac{(it)^n}{n!} \mathcal{L}^n \hat{O}, \quad (2)$$

where the second equality results from Baker-Campbell-Hausdorff formula. This expression in-

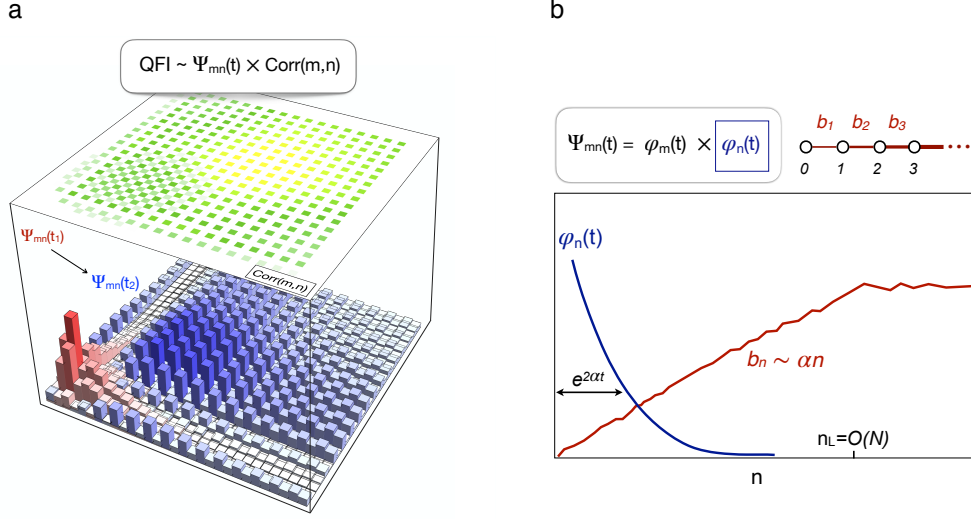


FIG. 1. **QFI evolution and exponentially fast entanglement generation from quantum delocalization picture.** (a) The QFI evolution can be interpreted as delocalizing a 2D wavefunction, $\Psi_{mn}(t) = \varphi_m(t)\varphi_n(t)$, on a correlation landscape denoted by $\text{Corr}(m, n)$. It reaches the optimum when the main population of $\Psi_{mn}(t)$ evolves to the local maximum of $\text{Corr}(m, n)$, i.e. marked by the light yellow region. (b) In Krylov space, the 1D component dynamics of $\Psi_{mn}(t)$ corresponds to quantum delocalization on a semi-infinite chain governed by a set of hopping amplitudes $\{b_n\}$. For many-body systems with a linearly increasing hopping amplitudes (i.e. $b_n \sim \alpha n$), a compelling exponentially fast delocalization of $\varphi_n(t)$ occurs with a spreading length of $\sim e^{2\alpha t}$. This characteristics is delicately connected to entanglement generation in an exponentially fast speed.

indicates that the operator evolution is confined in an operator subspace spanned by the recursively generated commutators $\{\hat{O}, \mathcal{L}\hat{O}, \mathcal{L}^2\hat{O}, \dots\}$. Supposing that the Hermitian operator set $\{\hat{O}_0, \hat{O}_1, \hat{O}_2, \dots\}$ forms an orthogonal basis of such a subspace, we are able to expand the time-evolved operator as

$$\hat{O}(t) = \sum_{n=0} \varphi_n(t) \hat{O}_n, \quad (3)$$

where the real coefficient vector, $[\varphi_0(t), \varphi_1(t), \varphi_2(t), \dots]^T$, represents an effective operator wavefunction that obeys a Schrödinger-type equation governed by the Liouvillian [38]. Its dynamics characterizes the delocalization of $\hat{O}(t)$ on a one-dimensional chain formed by $\{\hat{O}_n\}$. This basis can usually be interpreted as stratifying operators according to their “complexity”, where $\mathcal{L}^n \hat{O}$ becomes increasingly complex through recursive commutations with a many-body Hamiltonian. Physically, this process describes the generic delocalization of simple operators into an infinite

“bath” of increasingly nonlocal operators, a phenomenon known as operator growth [36, 56, 57].

As a major result of this work, we rigorously reformulate the general QFI evolution within this operator subspace as follows [38]

$$F_Q[\rho(t), \hat{O}] = 4 \sum_{m,n=0} \varphi_m(t)\varphi_n(t)\text{Corr}(m, n), \quad (4)$$

where $\text{Corr}(m, n)$ represents a correlation function between the basis operators \hat{O}_m and \hat{O}_n . Specifically, for an arbitrary pure initial state, it follows the form [38]

$$\text{Corr}(m, n) = \langle \hat{O}_m \hat{O}_n + \hat{O}_n \hat{O}_m \rangle / 2 - \langle \hat{O}_m \rangle \langle \hat{O}_n \rangle, \quad (5)$$

with the expectation $\langle \bullet \rangle$ taken with respect to the initial state. We define a 2D wavefunction, $\Psi_{mn}(t) = \varphi_m(t)\varphi_n(t)$, to characterize quantum delocalization along two orthogonal directions, each of which is independently quantified by the operator wavefunction. Thereby, the main result in Eq. (4) has a direct conceptual implication, unveiling an intriguing framework that the QFI dynamics can be generally interpreted as the delocalization of an effective wavefunction $\Psi_{mn}(t)$ on a correlation landscape characterized by $\text{Corr}(m, n)$, as shown by Fig. 1(a).

Guiding principle for identifying exponentially fast entanglement generation

We primarily focus on the common scenario where the nested commutators $\{\hat{O}, \mathcal{L}\hat{O}, \mathcal{L}^2\hat{O}, \dots\}$ fail to close, indicating the involvement of an infinite-dimensional Lie algebra. This situation typically arises in genuine interacting many-body Hamiltonians. Explicitly, we employ the Lanczos algorithm [39], which orthogonalizes $\{\mathcal{L}^n \hat{O}\}$ through a Gram-Schmidt procedure. The algorithm yields a sequence of positive numbers, $\{b_n\}$, known as Lanczos coefficients, and an orthogonal sequence of Hermitian operators, $\{i^n \hat{O}_n\}$, referred to as Krylov basis spanning the Krylov space. In this space, the Liouvillian takes the form of a tridiagonal matrix [38]:

$$\mathcal{L} = \begin{pmatrix} 0 & ib_1 & 0 & 0 & \cdots \\ -ib_1 & 0 & ib_2 & 0 & \cdots \\ 0 & -ib_2 & 0 & ib_3 & \cdots \\ 0 & 0 & -ib_3 & 0 & \ddots \\ \vdots & \vdots & \vdots & \ddots & \ddots \end{pmatrix}. \quad (6)$$

Straightforwardly, the operator wavefunction satisfies the following Schrödinger equation on a semi-infinite chain,

$$\partial_t \varphi_n = -b_{n+1} \varphi_{n+1} + b_n \varphi_{n-1}, \quad \varphi_n(0) = \delta_{n0}, \quad (7)$$

with $b_0 = \varphi_{-1} = 0$ by convention. Based on this equation, the universal properties of operator delocalization can be classified by different asymptotics of Lanczos coefficients [38]. A particularly intriguing case would be the linearly increasing one, namely $b_n \sim \alpha n$ for some real constant $\alpha > 0$. This case leads to an exponentially fast delocalization of $\varphi_n(t)$ in Krylov space, which is well characterized by a quantity called Krylov complexity to measure the expected position of $\varphi_n(t)$, namely $\mathcal{K}(t) = \sum_n n \varphi_n(t)^2 \sim e^{2\alpha t}$ [36]. Moreover, such a characteristics can also be captured by an approximate form of $|\varphi_n(t)| \sim e^{-n/\xi(t)}$ at large n , where $\xi(t) \sim e^{2\alpha t}$ is a delocalization length that grows exponentially in time, as shown by Fig. 1(b).

Importantly, Eq. (4) reveals that the dynamical behavior of the QFI is determined by the delocalization of the operator wavefunction and the feature of the correlation landscape. We consider a paradigm in which the diagonal part of $\text{Corr}(m, n)$ contributes dominantly to the QFI and exhibits a local maximum around a point (n^*, n^*) , as illustrated by the light yellow region in Fig. 1. This paradigm can be realized in various explicit scenarios and directly implies that the QFI reaches a local maximum when the main population of the operator wavefunction, $\varphi_n(t)$, arrives at the point $n = n^*$ in Krylov space. Based on the above analysis of operator delocalization, we can formulate the following proposition for identifying many-body interacting systems that enables exponentially fast entanglement generation.

Proposition: If the operator wavefunction $\varphi_n(t^*)$ at the evolution time $t = t^*$, when the QFI achieves its (local) maximum, is completely covered by the linearly increasing region of the Lanczos coefficients (denoted as $[0, n_L]$), the optimal evolution time would satisfy $t^* \simeq \log[\mathcal{K}(t^*)] \lesssim \log n_L \lesssim \log N$.

The last inequality in this proposition results from the fact that the linear region of Lanczos coefficients is usually up to the order of $n_L \lesssim O(N)$ for a N -particle system [58]. We also point out a criteria that if $n_L \gg n^*$, no significant population of $\varphi_n(t^*)$ would leak out of the region of $[0, n_L]$, by noticing the exponentially decay tail of $\varphi_n(t)$ on the n axis. This can be made more explicit, e.g. by requiring that $n_L/n^* \geq \nu$ with $\nu = 4$ [38]. We remark that such a proposition provides us a general guiding principle to find multipartite interacting systems that can create entanglement in an exponentially fast speed by deterministic Hamiltonian evolution. Specifically, we should engineer many-body Hamiltonians with linearly increasing Lanczos coefficients, such as the ones describing scrambling and chaotic quantum systems, which covers previously studied

explicit examples [6, 44, 59–63].

Entangling dynamics in Lipkin-Meshkov-Glick model

As an illustrative example, we consider the Lipkin-Meshkov-Glick (LMG) Hamiltonian [37],

$$\mathcal{H}_{\text{LMG}} = -\frac{\chi}{N} J_x^2 - \Omega J_z, \quad (8)$$

where $\mathbf{J} = (J_x, J_y, J_z)$ represents the total spin of the system comprised of N spin-1/2 particles. Starting from a coherent spin state pointing along the positive z -axis (i.e. $|\Psi\rangle = |\uparrow\uparrow \cdots \uparrow\rangle$), the system exhibits a saddle-point dominated scrambling dynamics at $\chi = 2\Omega$. The QFI blows up exponentially at initial times, and subsequently slows down to achieve the maximum, $F_Q[\rho(t), J_x] \approx 0.64N^2$, for an optimal evolution time $t = t^*$, see Fig. 2 (a). It can be seen that the operator wavefunction at the time t^* is almost fully located in the linearly increasing region of Lanczos coefficients [Fig. 2 (b)], indicating that a globally entangled state of $F_Q/N \sim O(N)$ is generated in an exponentially fast speed, namely $t^* \lesssim \log N$. We confirm this result by exact numerical fitting in Supplementary Materials [38].

Furthermore, we demonstrate that the intricate growth behavior of the QFI can be understood from the picture of quantum delocalization in correlation landscape. As shown by the explicit calculation of $\text{Corr}(m, n)$ in Fig. 2 (c), the diagonal stripe of the correlation landscape contributes dominantly to the QFI. We introduce the following quantity to characterize the feature of the correlation landscape,

$$f_n = 2 \sum_{m=n-w}^{n-1} \text{Corr}(m, n) + \text{Corr}(n, n), \quad (9)$$

where the integer w is properly chosen according to the stripe width. One can see in Fig. 2 (d) that f_n , depicted by the light green line, shows a linear increase up to a certain value of $n = n_c$. We take an average of f_n between adjacent sites to eliminate the strong fluctuations for large n , and denote it as $\bar{f}_n = (f_n + f_{n+1})/2$, which achieves a maximum at $n \approx n^*$. By further making a replacement of $\varphi_n(t)\varphi_m(t) \rightarrow \varphi_n^2(t)$ in Eq. (4) over the diagonal stripe, we can define a variant of the QFI to qualitatively capture its dynamical behavior from a 1D delocalization picture,

$$\mathcal{F}_Q = 4 \sum_{n=0}^{\infty} \bar{f}_n \varphi_n^2(t). \quad (10)$$

This formulation predicts that \mathcal{F}_Q is proportional to Krylov complexity and exhibits an exponential blow-up at initial times once $\varphi_n(t)$ is located in the region of $[0, n_c]$, namely $\sum_{n>n_c}^{\infty} \varphi_n(t)^2$ is

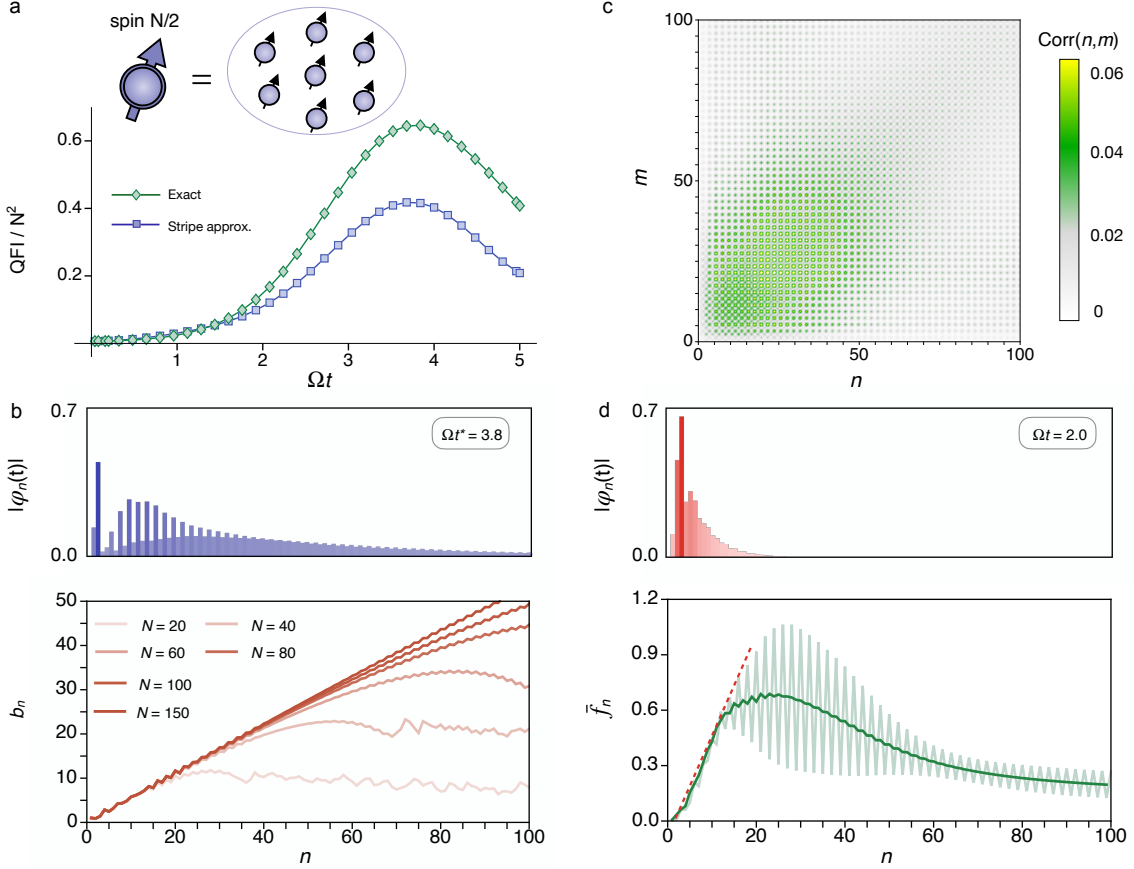


FIG. 2. Exponentially fast generation of global entanglement in LMG model. (a) The exact QFI and the QFI variant from the delocalization picture grow exponentially at transient times, and then slows down to achieve the optimum. (b) The Lanczos coefficients show a linear increase up to $n_L \simeq N$. At the time $t = t^* \approx 3.8/\Omega$ when the QFI is maximal, the main population of $\Psi_{mn}(t)$ reaches the dominant region of $\text{Corr}(m, n)$ around $m^* = n^* \approx 25$ in panel (c). The straightforward observation of $n_L \geq 5n^*$ leads to that $\varphi_n(t^*)$ is almost completely covered by $[0, n_L]$, indicating that the maximum of the QFI is achieved exponentially fast. (d) The reduced quantity \bar{f}_n from the dominant stripe of $\text{Corr}(m, n)$ increases linearly for $n \leq n_c \approx 12$, resulting in a transient exponential blow-up of $\mathcal{F}_Q(t)$ as long as $\varphi_n(t)$ is fully located in the region of $[0, n_c]$, i.e. approximately before the time $t = 2/\Omega$. We note that the values of $\text{Corr}(m, n)$ are rescaled by a factor of N^2 , the system size is set as $N = 150$, and the stripe width is chosen as $w = 10$.

negligible [see Fig. 2 (d)]. Beyond this region, the growth of \mathcal{F}_Q slows down and reaches its maximum when the main population of $\varphi_n(t)$ arrives the maximum of \bar{f}_n .

Exponentially fast entanglement generation in chaotic FP model

The present guiding principle points to versatile many-body systems with linearly increasing

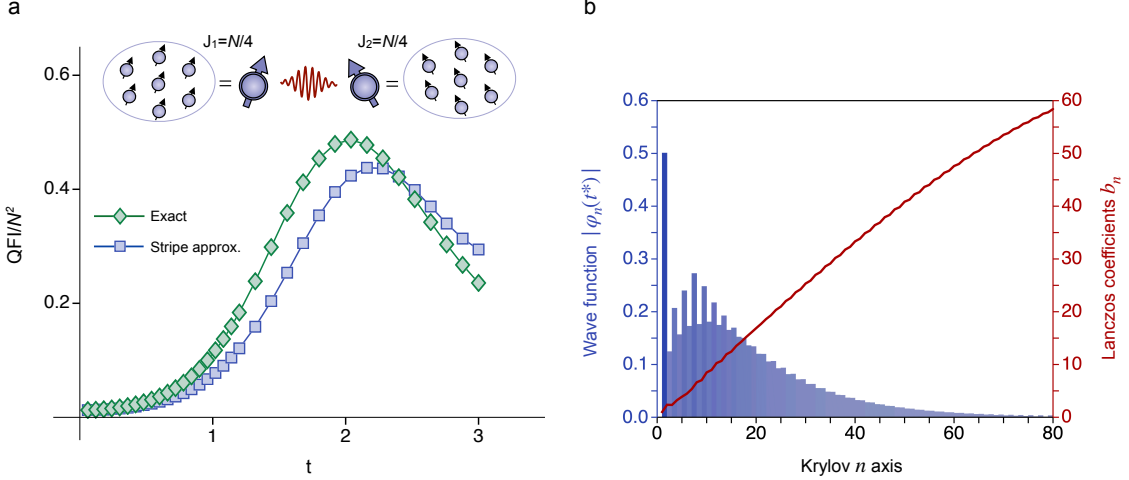


FIG. 3. **Exponentially fast generation of global entanglement in FP model.** (a) The exact QFI and its variant from 1D delocalization picture as defined in Eq. (10) exhibit similar behaviors, which grow exponentially at transient times and then slows down to achieve the optimum. (b) The operator wavefunction $\varphi_n(t^*)$ when the QFI achieves its maximum [$F_Q(t^*) \approx 0.48N^2$ at $t^* \approx 2.03$] is fully covered by the linearly increasing region of Lanczos coefficients, indicating an exponentially fast generation of a globally entangled state. Here, the system size is $N = 80$ and $J = N/4 = 20$, the stripe width is chosen as $w = 30$.

asymptotics of Lanczos coefficients for exponentially fast entanglement generation, with chaotic quantum systems as the most straightforward examples. A universal operator growth hypothesis states that an infinite, non-integrable, many-body system possesses an asymptotically linear Lanczos coefficients for an operator \hat{O} that has zero overlap with any conserved quantity [36]. As a well-studied model of quantum chaos, the Feingold-Peres (FP) model of coupled tops describes a system of two spin- J components, 1 and 2, of which the Hamiltonian is given by

$$\mathcal{H}_{\text{FP}} = (1 + c)(J_1^z + J_2^z) + \frac{4}{J}(1 - c)J_1^x J_2^x, \quad (11)$$

where the parameter $c \in [-1, 1]$ and the spin operators J_i^α satisfy the $SU(2)$ algebra $[J_i^\alpha, J_j^\beta] = i\delta_{ij}\epsilon_{\alpha\beta\gamma}J_i^\gamma$. It is noninteracting at $c = \pm 1$ and displays generic chaotic dynamics in the intermediate region [64]. Remarkably, this system has not been exploited to prepare multipartite entanglement. Here we find that, starting from the initial product state $|\Psi\rangle = |\uparrow\rangle^{\otimes N/2} \otimes |\uparrow\rangle^{\otimes N/2}$, the Lanczos coefficients at $c = 0$ increase linearly up to the order of the spin size [see Fig. 3 (a)]. An exponentially fast growth of the QFI associated with the interrogation operator $\hat{O} = J_1^x + J_2^x$ that has no overlap with the system Hamiltonian highlights applicability of the guiding principle [see Fig. 3 (b)]. Similar to the analysis in LMG model, we find that the QFI achieves its optimum

$F_Q \approx 0.48N^2$ at $t^* \lesssim \log(N)$, which achieves Heisenberg limit and might be utilized to efficiently construct two-partite quantum enhanced sensors [65]. This result is also verified by exact numerical fitting in Supplementary Materials [38].

Conclusion & outlook

To summarize, we have developed a comprehensive framework for quantifying the growth of multipartite entanglement in many-body systems by connecting the evolution of the QFI to quantum delocalization in an operator subspace. Using the efficient Krylov approach, we have established a link between the exponentially fast generation of multipartite entanglement and the universal characteristics of the linearly increasing Lanczos coefficients in generic chaotic or scrambling Hamiltonian systems. We remark that the general entangling dynamics in Eq. (4) is deeply connected to initial states involved in the correlation landscape. After identifying a multipartite interacting system, the subsequent construction of delicate optimization procedures to determine the optimal form of the initial state deserves intense efforts in future research. It should also be pointed out that the local-operator-related QFI might be blind to non-local entanglement embedded in the celebrated W states and topological phases [28]. A remain challenge is the question whether non-local extensions of the presented framework permit the efficient analysis of entanglement growth speed in relevant strategies [66, 67]. Other interesting directions include extending our framework to periodically driven chaotic systems [68, 69] as well as open quantum systems with decoherence [38], and exploring the potential of our results to identify signatures of rapidly generating macroscopic quantum states [7, 70]. The implications of our findings extend beyond the realm of fundamental quantum physics, as the ability to generate entanglement exponentially fast has far-reaching consequences for the development of cutting-edge quantum technologies.

Acknowledgements

This work is supported by the National Natural Science Foundation of China (12161141011 and 12174138), the National Key R&D Program of China (2018YFA0306600), and the Shanghai Key Laboratory of Magnetic Resonance (East China Normal University). Y.-M.C. is also supported by the Young Scientists Fund of the National Natural Science Foundation of China (12304572) and the fellowship of China Postdoctoral Science Foundation (2022M721256).

[1] Y. Lu, S. Zhang, K. Zhang, W. Chen, Y. Shen, J. Zhang, J.-N. Zhang, and K. Kim, Global entangling gates on arbitrary ion qubits, *Nature* **572**, 363 (2019).

- [2] Z. Eldredge, Z.-X. Gong, J. T. Young, A. H. Moosavian, M. Foss-Feig, and A. V. Gorshkov, Fast quantum state transfer and entanglement renormalization using long-range interactions, [Phys. Rev. Lett. **119**, 170503 \(2017\)](#).
- [3] M. Arndt and K. Hornberger, Testing the limits of quantum mechanical superpositions, [Nat. Phys. **10**, 271 \(2014\)](#).
- [4] M. Ardehali, Bell inequalities with a magnitude of violation that grows exponentially with the number of particles, [Phys. Rev. A **46**, 5375 \(1992\)](#).
- [5] L. Amico, R. Fazio, A. Osterloh, and V. Vedral, Entanglement in many-body systems, [Rev. Mod. Phys. **80**, 517 \(2008\)](#).
- [6] X. Zhang, Z. Hu, and Y.-C. Liu, Fast generation of GHZ-like states using collective-spin XYZ model, [Phys. Rev. Lett. **132**, 113402 \(2024\)](#).
- [7] F. Fröwis, P. Sekatski, W. Dür, N. Gisin, and N. Sangouard, Macroscopic quantum states: Measures, fragility, and implementations, [Rev. Mod. Phys. **90**, 025004 \(2018\)](#).
- [8] L. Pezzè, A. Smerzi, M. K. Oberthaler, R. Schmied, and P. Treutlein, Quantum metrology with non-classical states of atomic ensembles, [Rev. Mod. Phys. **90**, 035005 \(2018\)](#).
- [9] C. D. Marciniak, T. Feldker, I. Pogorelov, R. Kaubruegger, D. V. Vasilyev, R. van Bijnen, P. Schindler, P. Zoller, R. Blatt, and T. Monz, Optimal metrology with programmable quantum sensors, [Nature **603**, 604 \(2022\)](#).
- [10] E. Pedrozo-Peñafiel, S. Colombo, C. Shu, A. F. Adiyatullin, Z. Li, E. Mendez, B. Braverman, A. Kawasaki, D. Akamatsu, Y. Xiao, *et al.*, Entanglement on an optical atomic-clock transition, [Nature **588**, 414 \(2020\)](#).
- [11] G. P. Greve, C. Luo, B. Wu, and J. K. Thompson, Entanglement-enhanced matter-wave interferometry in a high-finesse cavity, [Nature **610**, 472 \(2022\)](#).
- [12] H. Bao, J. Duan, S. Jin, X. Lu, P. Li, W. Qu, M. Wang, I. Novikova, E. E. Mikhailov, K.-F. Zhao, K. Mølmer, H. Shen, and Y. Xiao, Spin squeezing of 10^{11} atoms by prediction and retrodiction measurements, [Nature **581**, 159 \(2020\)](#).
- [13] H. J. Briegel, D. E. Browne, W. Dür, R. Raussendorf, and M. Van den Nest, Measurement-based quantum computation, [Nat. Phys. **5**, 19 \(2009\)](#).
- [14] C. Song, K. Xu, H. Li, Y.-R. Zhang, X. Zhang, W. Liu, Q. Guo, Z. Wang, W. Ren, J. Hao, H. Feng, H. Fan, D. Zheng, D.-W. Wang, H. Wang, and S.-Y. Zhu, Generation of multicomponent atomic Schrödinger cat states of up to 20 qubits, [Science **365**, 574 \(2019\)](#).

- [15] A. Omran, H. Levine, A. Keesling, G. Semeghini, T. T. Wang, S. Ebadi, H. Bernien, A. S. Zibrov, H. Pichler, S. Choi, J. Cui, M. Rossignolo, P. Rembold, S. Montangero, T. Calarco, M. Endres, M. Greiner, V. Vuletić, and M. D. Lukin, Generation and manipulation of Schrödinger cat states in Rydberg atom arrays, [Science](#) **365**, 570 (2019).
- [16] M. Hillery, V. Bužek, and A. Berthiaume, Quantum secret sharing, [Phys. Rev. A](#) **59**, 1829 (1999).
- [17] Z. Zhao, Y.-A. Chen, A.-N. Zhang, T. Yang, H. J. Briegel, and J.-W. Pan, Experimental demonstration of five-photon entanglement and open-destination teleportation, [Nature](#) **430**, 54 (2004).
- [18] S. Wehner, D. Elkouss, and R. Hanson, Quantum internet: A vision for the road ahead, [Science](#) **362**, eaam9288 (2018).
- [19] M. C. Tran, A. Y. Guo, A. Deshpande, A. Lucas, and A. V. Gorshkov, Optimal state transfer and entanglement generation in power-law interacting systems, [Phys. Rev. X](#) **11**, 031016 (2021).
- [20] H.-L. Shi, X.-W. Guan, and J. Yang, Universal shot-noise limit for quantum metrology with local Hamiltonians, [Phys. Rev. Lett.](#) **132**, 100803 (2024).
- [21] Y. Chu, X. Li, and J. Cai, Strong quantum metrological limit from many-body physics, [Phys. Rev. Lett.](#) **130**, 170801 (2023).
- [22] M. C. Tran, A. Y. Guo, C. L. Baldwin, A. Ehrenberg, A. V. Gorshkov, and A. Lucas, Lieb-Robinson light cone for power-law interactions, [Phys. Rev. Lett.](#) **127**, 160401 (2021).
- [23] A. Y. Guo, M. C. Tran, A. M. Childs, A. V. Gorshkov, and Z.-X. Gong, Signaling and scrambling with strongly long-range interactions, [Phys. Rev. A](#) **102**, 010401 (2020).
- [24] S. L. Braunstein and C. M. Caves, Statistical distance and the geometry of quantum states, [Phys. Rev. Lett.](#) **72**, 3439 (1994).
- [25] G. Tóth and I. Apellaniz, Quantum metrology from a quantum information science perspective, [J. Phys. A: Math. Theor.](#) **47**, 424006 (2014).
- [26] P. Hyllus, W. Laskowski, R. Krischek, C. Schwemmer, W. Wieczorek, H. Weinfurter, L. Pezzé, and A. Smerzi, Fisher information and multiparticle entanglement, [Phys. Rev. A](#) **85**, 022321 (2012).
- [27] G. Tóth, Multipartite entanglement and high-precision metrology, [Phys. Rev. A](#) **85**, 022322 (2012).
- [28] P. Hauke, M. Heyl, L. Tagliacozzo, and P. Zoller, Measuring multipartite entanglement through dynamic susceptibilities, [Nat. Phys.](#) **12**, 778 (2016).
- [29] O. Gühne and G. Tóth, Entanglement detection, [Phys. Rep.](#) **474**, 1 (2009).
- [30] I. Apellaniz, M. Kleinmann, O. Gühne, and G. Tóth, Optimal witnessing of the quantum Fisher information with few measurements, [Phys. Rev. A](#) **95**, 032330 (2017).

- [31] B. Swingle, Unscrambling the physics of out-of-time-order correlators, [Nat. Phys. **14**, 988 \(2018\)](#).
- [32] M. Rigol, V. Dunjko, and M. Olshanii, Thermalization and its mechanism for generic isolated quantum systems, [Nature **452**, 854 \(2008\)](#).
- [33] C. W. von Keyserlingk, T. Rakovszky, F. Pollmann, and S. L. Sondhi, Operator hydrodynamics, OTOCs, and entanglement growth in systems without conservation laws, [Phys. Rev. X **8**, 021013 \(2018\)](#).
- [34] T. Rakovszky, F. Pollmann, and C. W. von Keyserlingk, Diffusive hydrodynamics of out-of-time-ordered correlators with charge conservation, [Phys. Rev. X **8**, 031058 \(2018\)](#).
- [35] V. Khemani, A. Vishwanath, and D. A. Huse, Operator spreading and the emergence of dissipative hydrodynamics under unitary evolution with conservation laws, [Phys. Rev. X **8**, 031057 \(2018\)](#).
- [36] D. E. Parker, X. Cao, A. Avdoshkin, T. Scaffidi, and E. Altman, A universal operator growth hypothesis, [Phys. Rev. X **9**, 041017 \(2019\)](#).
- [37] B. Bhattacharjee, X. Cao, P. Nandy, and T. Pathak, Krylov complexity in saddle-dominated scrambling, [J. High Energ. Phys. **2022**, 174](#).
- [38] See Supplementary Materials at [link] for additional details of derivation and calculation, which include Refs.[8, 36, 39–55].
- [39] P. Caputa, J. M. Magan, and D. Patramanis, Geometry of Krylov complexity, [Phys. Rev. Res. **4**, 013041 \(2022\)](#).
- [40] S. Pang and T. A. Brun, Quantum metrology for a general Hamiltonian parameter, [Phys. Rev. A **90**, 022117 \(2014\)](#).
- [41] Y. Chu, S. Zhang, B. Yu, and J. Cai, Dynamic framework for criticality-enhanced quantum sensing, [Phys. Rev. Lett. **126**, 010502 \(2021\)](#).
- [42] C. Hotter, H. Ritsch, and K. Gietka, Combining critical and quantum metrology, [Phys. Rev. Lett. **132**, 060801 \(2024\)](#).
- [43] K. Gietka, L. Ruks, and T. Busch, Understanding and improving critical metrology. Quenching super-radiant light-matter systems beyond the critical point, [Quantum **6**, 700 \(2022\)](#).
- [44] Z. Li, S. Colombo, C. Shu, G. Velez, S. Pilatowsky-Cameo, R. Schmied, S. Choi, M. Lukin, E. Pedrozo-Peñafiel, and V. Vuletić, Improving metrology with quantum scrambling, [Science **380**, 1381 \(2023\)](#).
- [45] B. Yurke, S. L. McCall, and J. R. Klauder, SU(2) and SU(1,1) interferometers, [Phys. Rev. A **33**, 4033 \(1986\)](#).

- [46] C. Gross, T. Zibold, E. Nicklas, J. Estève, and M. K. Oberthaler, Nonlinear atom interferometer surpasses classical precision limit, [Nature](#) **464**, 1165 (2010).
- [47] Q. Liu, L.-N. Wu, J.-H. Cao, T.-W. Mao, X.-W. Li, S.-F. Guo, M. K. Tey, and L. You, Nonlinear interferometry beyond classical limit enabled by cyclic dynamics, [Nat. Phys.](#) **18**, 167 (2022).
- [48] M.-J. Hwang, R. Puebla, and M. B. Plenio, Quantum phase transition and universal dynamics in the Rabi model, [Phys. Rev. Lett.](#) **115**, 180404 (2015).
- [49] M. Gabrielli, L. Pezzè, and A. Smerzi, Spin-mixing interferometry with Bose-Einstein condensates, [Phys. Rev. Lett.](#) **115**, 163002 (2015).
- [50] V. Subramanyan, S. S. Hegde, S. Vishveshwara, and B. Bradlyn, Physics of the inverted harmonic oscillator: From the lowest Landau level to event horizons, [Ann. Phys.](#) **435**, 168470 (2021).
- [51] J. Vidal, G. Palacios, and C. Aslangul, Entanglement dynamics in the Lipkin-Meshkov-Glick model, [Phys. Rev. A](#) **70**, 062304 (2004).
- [52] S. Dusuel and J. Vidal, Finite-size scaling exponents of the Lipkin-Meshkov-Glick model, [Phys. Rev. Lett.](#) **93**, 237204 (2004).
- [53] S. Dusuel and J. Vidal, Continuous unitary transformations and finite-size scaling exponents in the Lipkin-Meshkov-Glick model, [Phys. Rev. B](#) **71**, 224420 (2005).
- [54] C. Liu, H. Tang, and H. Zhai, Krylov complexity in open quantum systems, [Phys. Rev. Res.](#) **5**, 033085 (2023).
- [55] J. T. Reilly, J. D. Wilson, S. B. Jäger, C. Wilson, and M. J. Holland, Optimal generators for quantum sensing, [Phys. Rev. Lett.](#) **131**, 150802 (2023).
- [56] A. Nahum, S. Vijay, and J. Haah, Operator spreading in random unitary circuits, [Phys. Rev. X](#) **8**, 021014 (2018).
- [57] T. Schuster and N. Y. Yao, Operator growth in open quantum systems, [Phys. Rev. Lett.](#) **131**, 160402 (2023).
- [58] J. Barbón, E. Rabinovici, R. Shir, and R. Sinha, On the evolution of operator complexity beyond scrambling, [J. High Energ. Phys.](#) **2019**, 264.
- [59] M. Kitagawa and M. Ueda, Squeezed spin states, [Phys. Rev. A](#) **47**, 5138 (1993).
- [60] A. Micheli, D. Jaksch, J. I. Cirac, and P. Zoller, Many-particle entanglement in two-component Bose-Einstein condensates, [Phys. Rev. A](#) **67**, 013607 (2003).
- [61] D. Kajtoch and E. Witkowska, Quantum dynamics generated by the two-axis countertwisting Hamiltonian, [Phys. Rev. A](#) **92**, 013623 (2015).

- [62] W. Muessel, H. Strobel, D. Linnemann, T. Zibold, B. Juliá-Díaz, and M. K. Oberthaler, Twist-and-turn spin squeezing in Bose-Einstein condensates, [Phys. Rev. A **92**, 023603 \(2015\)](#).
- [63] M. H. Muñoz Arias, I. H. Deutsch, and P. M. Poggi, Phase-space geometry and optimal state preparation in quantum metrology with collective spins, [PRX Quantum **4**, 020314 \(2023\)](#).
- [64] Y. Fan, S. Gnutzmann, and Y. Liang, Quantum chaos for nonstandard symmetry classes in the Feingold-Peres model of coupled tops, [Phys. Rev. E **96**, 062207 \(2017\)](#).
- [65] R. Kaubruegger, A. Shankar, D. V. Vasilyev, and P. Zoller, Optimal and variational multiparameter quantum metrology and vector-field sensing, [PRX Quantum **4**, 020333 \(2023\)](#).
- [66] S. Bugu, C. Yesilyurt, and F. Ozaydin, Enhancing the W-state quantum-network-fusion process with a single Fredkin gate, [Phys. Rev. A **87**, 032331 \(2013\)](#).
- [67] F. Ozaydin, C. Yesilyurt, S. Bugu, and M. Koashi, Deterministic preparation of W states via spin-photon interactions, [Phys. Rev. A **103**, 052421 \(2021\)](#).
- [68] J. T. Reilly, S. B. Jäger, J. D. Wilson, J. Cooper, S. Eggert, and M. J. Holland, Speeding up squeezing with a periodically driven Dicke model, [Phys. Rev. Res. **6**, 033090 \(2024\)](#).
- [69] W. Liu, M. Zhuang, B. Zhu, J. Huang, and C. Lee, Quantum metrology via chaos in a driven Bose-Josephson system, [Phys. Rev. A **103**, 023309 \(2021\)](#).
- [70] F. Fröwis and W. Dür, Measures of macroscopicity for quantum spin systems, [New J. Phys. **14**, 093039 \(2012\)](#).

Supplementary Materials

Yaoming Chu,¹ Xiangbei Li,¹ and Jianming Cai^{1,*}

*¹School of Physics, Hubei Key Laboratory of Gravitation and Quantum Physics,
International Joint Laboratory on Quantum Sensing and Quantum Metrology,
Institute for Quantum Science and Engineering,
Huazhong University of Science and Technology, Wuhan 430074, China*

Supplementary Section

- I. QFI dynamics in Krylov space
- II. Exponential fast delocalization on the correlation landscape
- III. Non-exponential fast delocalization on the correlation landscape
- IV. Transient exponential blow-up of QFI on finite-dimensional correlation landscape
- V. Full quantum analysis of atomic $SU(1, 1)$ approach in Krylov space
- VI. Effect of physical imperfections and decoherence
- VII. Optimal interrogation operator for the entangling dynamics

Supplementary Figures

- FIG. S1. Exponentially fast generation of global entanglement in LMG model
- FIG. S2. Extended materials for Feingold-Peres model
- FIG. S3. General delocalization behavior of the operator wavefunction in Krylov space
- FIG. S4. Linear delocalization of the operator wavefunction in OAT model
- FIG. S5. Diagonal behaviors of the correlation landscape $\text{Corr}(n, m)$ in OAT model
- FIG. S6. Exact QFI dynamics and saturation time in OAT model
- FIG. S7. QFI dynamics and its behavior in Krylov space by $SU(1, 1)$ approach
- FIG. S8. Exponentially fast entanglement generation by $SU(1, 1)$ approach
- FIG. S9. Effect of physical imperfections of the Hamiltonian parameter in LMG model
- FIG. S10. Effect of physical imperfections of the unwanted transverse field in LMG model
- FIG. S11. Effect of decoherence in LMG model
- FIG. S12. Correlated behaviors between the exact and approximated QFI in LMG model

I. QFI dynamics in Krylov space

In this section, we provide a detailed derivation of QFI dynamics in the Krylov space. The Taylor expression of the time-evolved interrogation operator, $\hat{\mathcal{O}}(t) = e^{i\mathcal{L}t}\hat{\mathcal{O}} = \sum_{n=0}^{\infty} (it)^n \mathcal{L}^n \hat{\mathcal{O}}/n!$, shows that the operator dynamics can be solved in a vectorized linear space spanned by the nested commutators $\{\hat{\mathcal{O}}, \mathcal{L}\hat{\mathcal{O}}, \mathcal{L}^2\hat{\mathcal{O}}, \dots\}$. To highlight the vector space structure, we make use of the bracket notation $|\mathcal{O}\rangle$ to regard the operator as a state in the Hilbert space of operators. Such an operator subspace can be equipped with an infinite-temperature inner product,

$$\langle \mathcal{O}_1 | \mathcal{O}_2 \rangle := \frac{1}{\mathcal{N}} \text{tr}(\hat{\mathcal{O}}_1^\dagger \hat{\mathcal{O}}_2) \quad (\text{S.1})$$

where \mathcal{N} is a constant normalization factor, for example, one can choose $\mathcal{N} = \text{tr}(\hat{\mathbb{1}})$ with $\hat{\mathbb{1}}$ the identity operator of the system. Besides, we write $\|\mathcal{O}\| := (\mathcal{O}|\mathcal{O})^{1/2}$ for the norm. Based on these notations, starting from normalized vectors $|\tilde{\mathcal{O}}_0\rangle := |\mathcal{O}\rangle/\|\mathcal{O}\|$ and $|\tilde{\mathcal{O}}_1\rangle := \mathcal{L}|\tilde{\mathcal{O}}_0\rangle/b_1$ with $b_1 = \|\mathcal{L}\tilde{\mathcal{O}}_0\|$, the Lanczos algorithm is defined by [1]

$$|A_n\rangle := \mathcal{L}|\tilde{\mathcal{O}}_{n-1}\rangle - b_{n-1}|\tilde{\mathcal{O}}_{n-2}\rangle, \quad b_n = \|A_n\|, \quad |\tilde{\mathcal{O}}_n\rangle := |A_n\rangle/b_n. \quad (\text{S.2})$$

The output of this algorithm is a set of real positive Lanczos coefficients $\{b_n\}$ and the orthonormal Krylov basis $\{|\tilde{\mathcal{O}}_n\rangle\}$, with $i^n \tilde{\mathcal{O}}_n$ being Hermitian. For simplicity, below we rescale this basis by a factor of $\|\mathcal{O}\|$, namely $\mathcal{O}_n = \|\mathcal{O}\| \tilde{\mathcal{O}}_n$. We note that the Krylov basis $\{|\mathcal{O}_n\rangle\}$ spans the so-called Krylov space containing $\hat{\mathcal{O}}(t)$ for any evolution time t , but does not usually span the full space of operators. The Liouvillian superoperator is tridiagonal in this basis (i.e. $\{i^n |\mathcal{O}_n\rangle\}$)

$$\mathcal{L} = \begin{pmatrix} 0 & ib_1 & 0 & 0 & \dots \\ -ib_1 & 0 & ib_2 & 0 & \dots \\ 0 & -ib_2 & 0 & ib_3 & \dots \\ 0 & 0 & -ib_3 & 0 & \ddots \\ \vdots & \vdots & \vdots & \ddots & \ddots \end{pmatrix}. \quad (\text{S.3})$$

Exploiting a linear expansion of the time-evolved operator in the Krylov space, i.e. $\hat{\mathcal{O}}(t) = \sum_{n=0}^{\infty} i^n \varphi_n(t) \hat{\mathcal{O}}_n$, the Heisenberg equation governed by the Liouvillian can be formulated as a discrete Schrödinger equation on a semi-infinite chain,

$$\partial_t \vec{\varphi} = i\mathcal{L}\vec{\varphi}, \quad \partial_t \varphi_n = -b_{n+1}\varphi_{n+1} + b_n\varphi_{n-1}, \quad \varphi_n(0) = \delta_{n0}, \quad (\text{S.4})$$

where $b_0 = \varphi_{-1} = 0$ by convention.

By further taking advantage of the connection between the QFI and the time-evolved interrogation operator revealed by Eq. (1) of the main text, the QFI dynamics during the state preparation stage can be reformulated as

$$F_Q[\rho(t), \hat{O}] = 4 \sum_{m,n=0}^{\infty} \varphi_m(t) \varphi_n(t) \text{Corr}(m, n). \quad (\text{S.5})$$

Here, $\text{Corr}(m, n)$ can be viewed as a real correlation landscape defined on Krylov basis, with an explicit formula as follows

$$\text{Corr}(m, n) = \frac{\gamma}{2} \text{tr} \left([i^m \hat{O}_m, \sqrt{\sigma}]^\dagger [i^n \hat{O}_n, \sqrt{\sigma}] \right). \quad (\text{S.6})$$

For the special case of pure-state metrology (i.e. $\sigma = |\Psi\rangle\langle\Psi|$ represents a pure state), we have $\gamma = 1$. Thereby, the above definition recovers an explicit form of correlation function given by Eq. (4) of the main text, namely

$$\text{Corr}(m, n) = \langle \hat{O}_m \hat{O}_n + \hat{O}_n \hat{O}_m \rangle / 2 - \langle \hat{O}_m \rangle \langle \hat{O}_n \rangle. \quad (\text{S.7})$$

Generally, the size of the Krylov basis operator gradually grows by recursive commutation with the system Hamiltonian [2]. Considering the common two-body interactions, for example, $H \sim \frac{1}{N} \sum_{\alpha\beta} J_\alpha J_\beta$ with $J_\alpha = \sum_{i=1}^N \sigma_\alpha^i$ denoting the collective spin operator and $\alpha, \beta = x, y, z$. Starting from an interrogation operator $\hat{O} = J_\alpha$, the possible highest order of the Krylov basis takes the form of

$$\hat{O}_{n-1} \sim \frac{1}{N^{n-1}} J_{\alpha_1} J_{\alpha_2} \cdots J_{\alpha_n} = \frac{1}{N^{n-1}} \sum_{i_1=1}^N \sigma_{\alpha_1}^{i_1} \sum_{i_2=1}^N \sigma_{\alpha_2}^{i_2} \cdots \sum_{i_n=1}^N \sigma_{\alpha_n}^{i_n}. \quad (\text{S.8})$$

The correlation landscape contributed by this part is then given by

$$\begin{aligned} \text{Corr}(m-1, n-1) \sim & \frac{1}{N^{m+n-2}} \sum_{i_1, i_2, \dots, i_n, j_1, j_2, \dots, j_m} \left[\langle \sigma_{\alpha_1}^{i_1} \sigma_{\alpha_2}^{i_2} \cdots \sigma_{\alpha_n}^{i_n} \sigma_{\beta_1}^{j_1} \sigma_{\beta_2}^{j_2} \cdots \sigma_{\beta_m}^{j_m} \rangle \right. \\ & \left. - \langle \sigma_{\alpha_1}^{i_1} \sigma_{\alpha_2}^{i_2} \cdots \sigma_{\alpha_n}^{i_n} \rangle \langle \sigma_{\beta_1}^{j_1} \sigma_{\beta_2}^{j_2} \cdots \sigma_{\beta_m}^{j_m} \rangle \right]. \end{aligned} \quad (\text{S.9})$$

We note that the number of the above summation terms equals to N^{m+n} , which is consistent with the fact that $\text{Corr}(m, n) \lesssim N^2$ due to the normalization, e.g. $\|\hat{O}_m\| = \|\hat{O}_n\| = \|\hat{O}\| \sim N$. In the Pauli string $\sigma_{\alpha_1}^{i_1} \sigma_{\alpha_2}^{i_2} \cdots \sigma_{\alpha_n}^{i_n} \sigma_{\beta_1}^{j_1} \sigma_{\beta_2}^{j_2} \cdots \sigma_{\beta_m}^{j_m}$, if no identical spins appears, the non-entangled feature of the initial state would lead to that

$$\langle \sigma_{\alpha_1}^{i_1} \sigma_{\alpha_2}^{i_2} \cdots \sigma_{\alpha_n}^{i_n} \sigma_{\beta_1}^{j_1} \sigma_{\beta_2}^{j_2} \cdots \sigma_{\beta_m}^{j_m} \rangle - \langle \sigma_{\alpha_1}^{i_1} \sigma_{\alpha_2}^{i_2} \cdots \sigma_{\alpha_n}^{i_n} \rangle \langle \sigma_{\beta_1}^{j_1} \sigma_{\beta_2}^{j_2} \cdots \sigma_{\beta_m}^{j_m} \rangle = 0. \quad (\text{S.10})$$

The number of such a configuration (i.e. no identical spins appearing) is given by

$$\begin{aligned}
\mathcal{N} &= N \times (N-1) \times (N-m-n+1) \\
&= N^{m+n} \left(1 - \frac{1}{N}\right) \cdots \left(1 - \frac{m+n-1}{N}\right) \\
&\geq N^{m+n} \left[\left(1 - \frac{1}{N}\right) \left(1 - \frac{m+n-1}{N}\right) \right]^{\frac{m+n}{2}} \\
&\geq N^{m+n} \left(1 - \frac{m+n}{N}\right)^{\frac{m+n}{2}}
\end{aligned} \tag{S.11}$$

Defining $(m+n)/2 = k$ and $(m+n)/N = \epsilon$, we can rewrite \mathcal{N} as follows

$$\mathcal{N}/N^{m+n} \geq (1-\epsilon)^k = 1 - k\epsilon + C_k^2 \epsilon^2 - C_k^3 \epsilon^3 + \dots \tag{S.12}$$

If $k\epsilon \ll 1$, $\mathcal{N} \geq N^{m+n}(1 - k\epsilon)$. This result implies that the maximal number of terms that give rise to non-zero result in Eq. (S.9) is smaller than $k\epsilon N^{m+n}$, which subsequently leads to that

$$\text{Corr}(m-1, n-1) \lesssim k\epsilon N^2 \simeq \frac{(m+n)^2}{N} N^2 \text{ and } \text{Corr}(n-1, n-1) \lesssim n^2 N \tag{S.13}$$

On the contrary, $\text{Corr}(n, n) \sim N^2$ would require that $k\epsilon \sim O(1)$ and thus $n \gtrsim \sqrt{N}$. This is deeply related to that the QFI achieves the Heisenberg scaling with respect to the initial product state. We point out that such a similar argument can be extended to short-range interaction as well.

II. Exponential fast delocalization on the correlation landscape

Next, we analyze the universal delocalization properties of the 1D operator wavefunction governed by Eq. (S.4), when the Lanczos coefficients take an asymptotically linear form, i.e. $b_n = \alpha n + \gamma + o(1)$. Specifically, we employ a family of exact solutions where

$$b_n = \alpha \sqrt{n(n-1+\eta)} \quad \rightarrow \quad b_n = \alpha n + \gamma \quad \text{for } n \gg 1. \tag{S.14}$$

In this case, the time-evolved operator wavefunction is analytically given by [1]

$$\varphi_n(t) = \sqrt{\frac{\Gamma(n+\eta) \tanh^n(\alpha t)}{n! \Gamma(\eta) \cosh^\eta(\alpha t)}}, \tag{S.15}$$

where $\Gamma(\bullet)$ represents the Gamma function and $\Gamma(n) = (n-1)!$ for an integer n . As a central consequence of the linearly increased Lanczos coefficients, the operator wavefunction delocalizes in an exponentially fast speed, which can be reflected in the expected position of $\varphi_n(t)$ on the semi-infinite chain, namely

$$\mathcal{K}(t) := \sum_{n=0}^{\infty} n \varphi_n^2(t) = \eta \sinh^2(\alpha t) \sim e^{2\alpha t}. \tag{S.16}$$

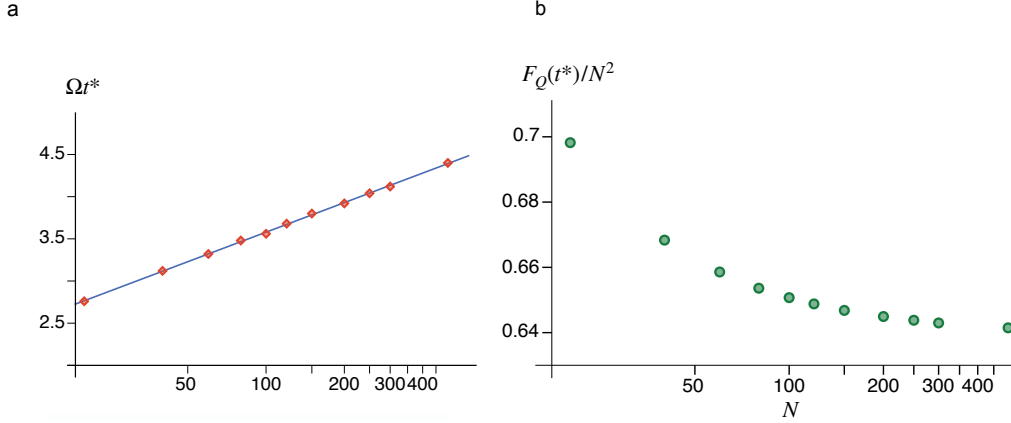


FIG. S1. **Exponentially fast generation of global entanglement in LMG model.** (a) The evolution time t^* at which the QFI achieves its maximum shows a logarithmic relation with the system size as $\Omega t^* \approx 0.51 \log N + 1.25$. (b) The maximal QFI at the time t^* approximately saturates to $F_Q(t^*) \approx 0.64N^2$ in the large- N limit. The system parameter is set as $\chi = 2\Omega = 2$.

This quantity is also known as the Krylov complexity characterizing nonequilibrium quantum many-body dynamics, by noticing the fact that the basis operator \hat{O}_n becomes increasingly complex (e.g. nonlocal) with n .

Below, we investigate the QFI dynamics based on Eq. (S.5), by focusing on the above exponential delocalization of the operator wavefunction on the correlation landscape. Without loss of generality, we set $\eta = 1$ and utilize a simple form of the wavefunction, namely $\varphi_n(t) = \tanh^n(\alpha t) / \cosh(\alpha t)$. Consider that the correlation landscape is dominated by its diagonal stripe, and exhibits the (first local) maximum around the point (n^*, n^*) . Intuitively, the QFI achieves the corresponding optimum at a specific evolution time t^* , when the main population of the operator wavefunction approaches this point. Such a condition can be mathematically quantified by the following equation

$$p^* = \sum_{n=0}^{n^*} \varphi_n^2(t^*) = 1 - [\tanh(\alpha t^*)]^{2n^*+2}, \quad (\text{S.17})$$

where we can roughly set $p^* = 1/2$, to indicate that the main population of $\varphi_n(t)$ reaches $n = n^*$ on the Krylov semi-infinite chain. More accurately, the deviations of the first few small Lanczos coefficients from the ideal asymptotics (i.e. $b_n = \alpha n$) might have an impact on the choice of p^* , by affecting the fraction of the population that can delocalize on Krylov axis. Particularly, if the first few Lanczos coefficients are relatively small as compared to the ideal ones, there might be a residual fraction of the population that always stays in the first few sites and fails to contribute

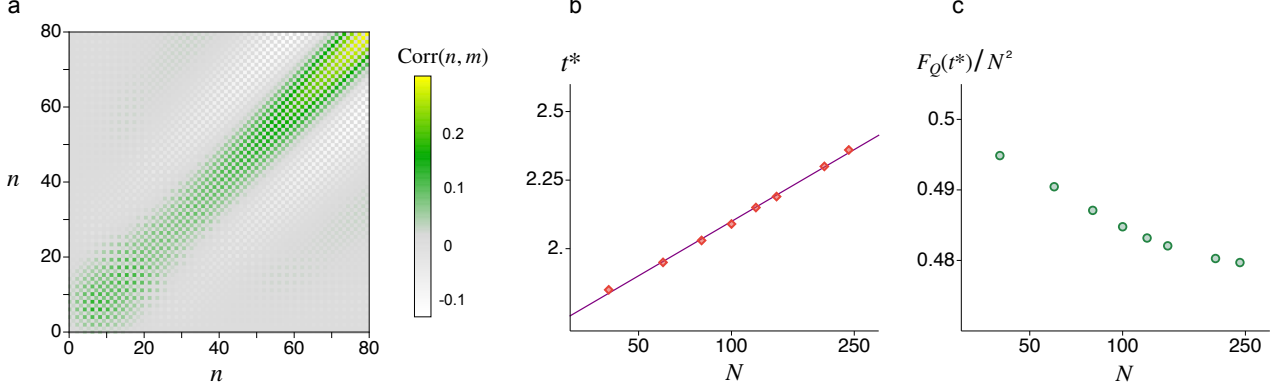


FIG. S2. **Extended materials for Feingold-Peres model.** (a) The correlation landscape is dominated by its diagonal stripe and exhibit the first local maximum around $(n^*, n^*) \approx (10, 10)$ for the system size $N = 80$. Combined with Fig. 3 in the main text, one can find that $n_L \gtrsim 4n^*$ with n_L characterizing the linearly increased region of the Lanczos coefficients. This implies an exponentially fast generation of global multipartite entanglement. (b) The evolution time t^* at which the QFI achieves its optimum shows a relation with the system size as $t^* \approx 0.29 \log N + 0.78$. (c) The maximal QFI at the time t^* approximately saturates to $F_Q(t^*) \approx 0.48N^2$ in the large- N limit. The system parameter of FP model is chosen as $c = 0$.

to the QFI growth. The most extreme case, for example, is that $b_1 = 0$ and the population would always be trapped in the initial site. In explicit scenarios, we denote the residual fraction that does not delocalize by \mathcal{R} , and determine the optimal evolution time t^* by setting $p^* = \mathcal{R} + (1 - \mathcal{R})/2 = (1 + \mathcal{R})/2$ in Eq. (S.17).

For a finite many-body interacting system composed of N particles, the linearly increased region of the Lanczos coefficients is usually up to the order of $n_L \sim O(N)$. Before the optimal evolution time (i.e. $t = t^*$), in order to ensure an exponentially fast delocalization of the operator wavefunction—namely, $t^* \lesssim \log(N)$, we suppose that $\varphi_n(t)$ is almost fully located in the region of $[0, n_L]$, namely

$$p^{(L)} = \sum_{n=0}^{n_L} \varphi_n^2(t^*) = 1 - [\tanh(\alpha t^*)]^{2n_L+2} = 1 - (1 - p^*)^{(n_L+1)/(n^*+1)} \rightarrow 1. \quad (\text{S.18})$$

In other words, very small fraction of the population leaks out of $[0, n_L]$, which has negligible impact on exponentially fast delocalization of the operator wavefunction. This condition can be satisfied by requiring that

$$(n_L + 1)/(n^* + 1) \gg 1. \quad (\text{S.19})$$

Usually, we have $n_L \gg 1$ and $n^* \gg 1$. By setting $n_L \geq \nu n^*$ and taking $\nu = 4$ for example, one can

obtain that $p^{(L)}$ is close to unit.

III. Non-exponential fast delocalization on the correlation landscape

While focusing on the exponentially fast generation of multipartite entanglement in the main text due to its essential significance, we further discuss in this section the potential applications of our framework in non-exponential scenarios. Firstly, we study the general behaviors of operator delocalization governed by Lanczos coefficients of a generic asymptotic form $b_n = \alpha n^\delta$, i.e.

$$\partial_t \varphi_n(t) = -\alpha(n+1)^\delta \varphi_{n+1}(t) + \alpha n^\delta \varphi_{n-1}(t). \quad (\text{S.20})$$

This differential equation, by rescaling the time parameter as $t \rightarrow \alpha t$, is equivalent to

$$\partial_t \varphi_n(t) = -(n+1)^\delta \varphi_{n+1}(t) + n^\delta \varphi_{n-1}(t). \quad (\text{S.21})$$

Therefore, the value of the exponent δ determines universal behaviors of operator delocalization. Particularly: (i) At $\delta = 1$, exponentially fast delocalization happens and Krylov complexity grows as $\mathcal{K}(t) = \sum_n n \varphi_n(t)^2 \sim e^{2t}$. (ii) At $\delta = 1/2$ and $b_n = \sqrt{n}$, the delocalization dynamics is equivalent to a quantum harmonic oscillator starting from the vacuum state and driven by $H = i(a^\dagger - a)$, with a (a^\dagger) the standard bosonic annihilation (creation) operator. The time-evolved state is a coherent state, namely $|\alpha\rangle = D(\alpha)|0\rangle = e^{\alpha(a^\dagger - a)}|0\rangle$ with $\alpha = t$. Using such an analogy, the Krylov

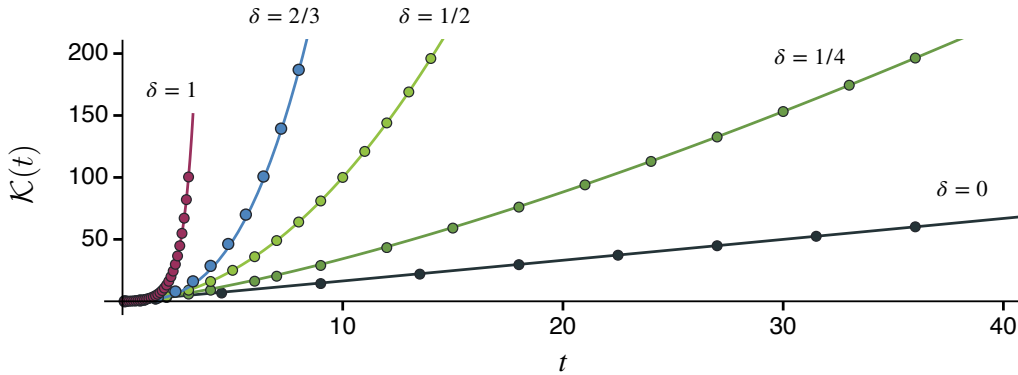


FIG. S3. **General delocalization behavior of the operator wavefunction in Krylov space.** The growth dynamics of Krylov complexity are numerically derived and then fitted for different values of the exponent δ . At $\delta = 1$, the fitting yields $\mathcal{K}(t) \approx 0.23e^{2.03t}$. For $\delta < 1$, we fit the dynamics by $\mathcal{K}(t) \approx at^\xi$ with $\{a, \xi\}$ equals to $\{0.5, 2.85\}$, $\{1, 2\}$, $\{1.5, 1.36\}$ and $\{1.59, 1.01\}$ for $\delta = 2/3$, $\delta = 1/2$, $\delta = 1/4$ and $\delta = 0$ respectively.

complexity is given by the mean excitation number of the harmonic oscillator, namely $\mathcal{K}(t) = |\alpha|^2 = t^2$. (iii) At $\delta = 0$ and $b_n = 1$, the coupling between neighboring sites on the semi-infinite Krylov chain is a constant. This would lead to a linear delocalization of the operator wavefunction, i.e. $\mathcal{K}(t) \sim t$. More values of δ are illustrated in Fig. S3 by numerical fitting. Based on the numerical results, below we assume that Krylov complexity for $b_n = n^\delta$ grows as $\mathcal{K}(t) \sim t^\xi$ with the exponent ξ depending on δ . More specifically, we have $\xi = 1/(1 - \delta)$ [2].

Similar to the proposition in the main text, if the operator wavefunction $\varphi_n(t^*)$ at the evolution time $t = t^*$, when the QFI achieves its (local) maximum, is completely covered by the asymptotic region (i.e. $b_n = n^\delta$) of the Lanczos coefficients (denoted as $[0, n_L]$), the optimal evolution time would satisfy

$$t^* \simeq [\mathcal{K}(t^*)]^{1/\xi} \lesssim n_L^{1/\xi} \lesssim N^{1/\xi}. \quad (\text{S.22})$$

On the other hand, by combining with the feature of the correlation landscape, for example, $\text{Corr}(n, n) \sim N^2$ requires that $n \gtrsim \sqrt{N}$, one could conjecture that a globally entangled state achieving the Heisenberg limit needs at least a generating time on the order of

$$t^* \gtrsim N^{\frac{1}{2\xi}}. \quad (\text{S.23})$$

As an illustrative example, we consider the paradigmatic one-axis-twisting (OAT) model for en-

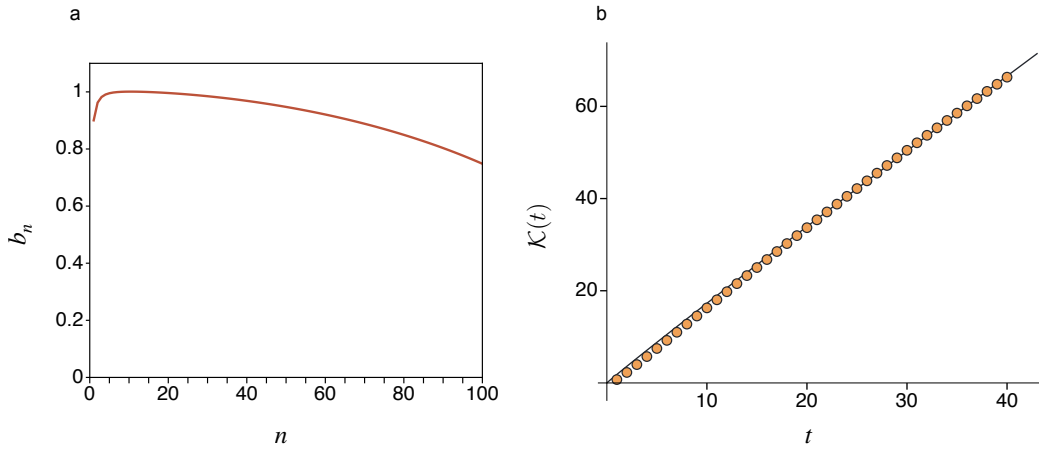


FIG. S4. **Linear delocalization of the operator wavefunction in OAT model.** (a) The Lanczos coefficients display no apparent growth and can be regarded as a constant. (b) The Krylov complexity grows linearly in time and can be well fitted by a function of $\mathcal{K}(t) \approx 1.84t^{0.97}$. Here, the system parameter is set as $\chi = 2$ and $N = 150$.

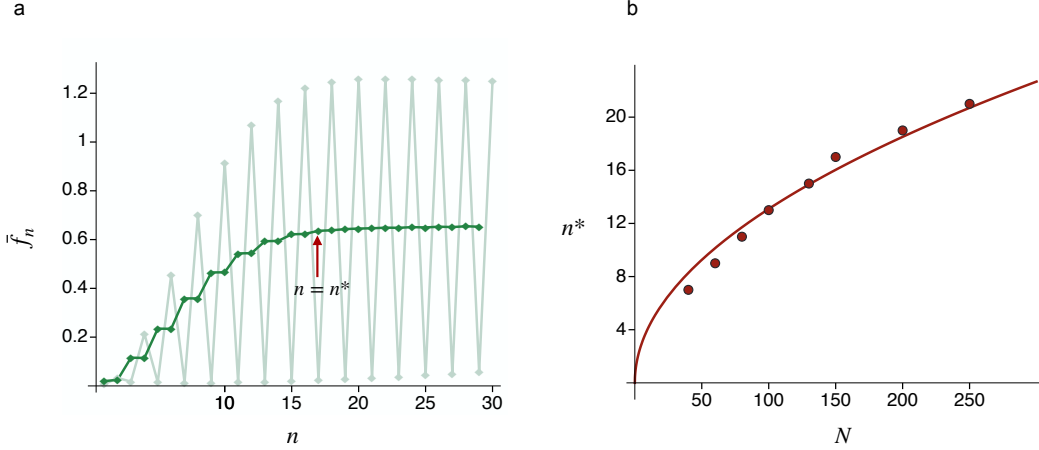


FIG. S5. **Diagonal behaviors of the correlation landscape** $\text{Corr}(n, m)$ **in OAT model.** (a) The quantity \bar{f}_n (rescaled by a factor of N^2) following from Eq. (9) in the main text firstly shows a linear increase and then saturates to a constant on the order of $O(1)$. Here the system size is set as $N = 150$. (b) The site n^* where \bar{f}_n starts to saturate approximately shows a square-root relation with the system size N , with the numerical fitting given by $n^* \approx 1.3\sqrt{N}$. The system parameter is set as $\chi = 2$.

tanglement generation [3], namely

$$\mathcal{H}_{\text{OAT}} = -\frac{\chi}{N} J_x^2. \quad (\text{S.24})$$

The initial state and interrogation operator is set as $|\Psi\rangle = |N/2\rangle = |\uparrow\uparrow \cdots \uparrow\rangle$ and $\hat{\mathcal{O}} = J_y$ respectively. As shown in Fig. S4, the Lanczos coefficients can be approximately viewed as a constant. This results in that the operator wavefunction delocalizes linearly in Krylov space. On the other hand, we find that the correlation landscape $\text{Corr}(m, n)$ is governed by its diagonal stripe. Hence, we characterize it using the quantity \bar{f}_n following from Eq. (9) in the main text, which initially shows a linear increase and then starts to saturate from a certain site $n^* \approx 1.3\sqrt{N}$, as can be seen in Fig. S5. Moreover, the saturation value \bar{f}_{n^*} is on the order of $O(1)$, indicating that the QFI of Heisenberg scaling (i.e. $F_Q \sim N^2$) might be achieved. Combining the above two aspects, namely the operator delocalization behavior and the feature of the correlation landscape, we conjecture that the QFI can saturate to $F_Q \simeq N^2$ from a certain time $t = t^* \sim \sqrt{N}$. This corresponds to that a global entanglement would be generated on the time scale of $t^* \sim \sqrt{N}$. We exactly verify this result in Fig. S6.

IV. Transient exponential blow-up of QFI on finite-dimensional correlation landscape

We also apply the present general framework based on quantum delocalization on correlation

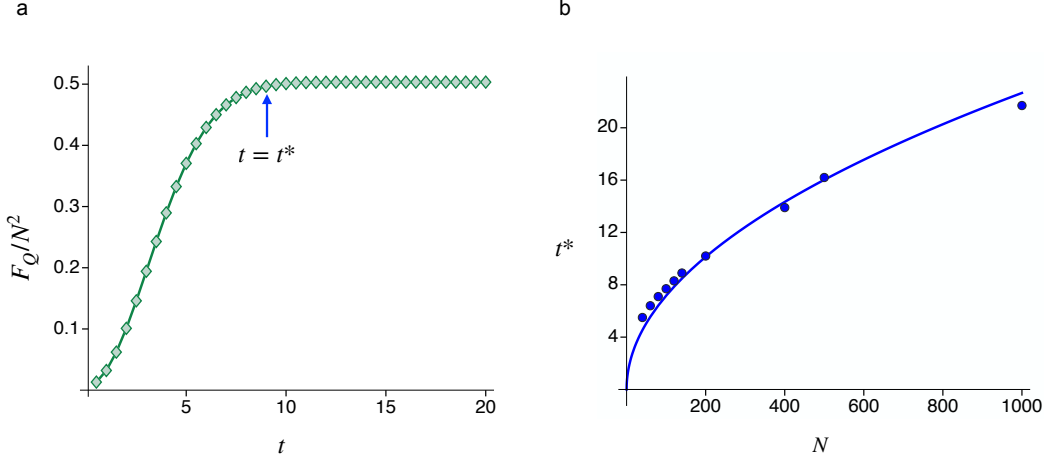


FIG. S6. **Exact QFI dynamics and saturation time in OAT model.** (a) The QFI saturates to the value of $F_Q \approx 0.5N^2$ from a certain time $t = t^*$. Here the system size is set as $N = 150$. (b) The saturation time t^* approximately shows a square-root relation with the system size N , namely $t^* \approx 0.7\sqrt{N}$. The system parameter is set as $\chi = 2$.

landscape to characterize the QFI evolution where the system Hamiltonian generates a closed Lie algebra with finite dimension [4, 5]. This involves several widely-used models in the quantum information context, including the well-known inverted harmonic oscillator (IHO) [6–8] and the $SU(1,1)$ interferometric approach [9–11]. We denote a basis of the finite Lie algebra as $\{\hat{O}_0, \hat{O}_1, \dots, \hat{O}_d\}$, satisfying a commutation relation $[\hat{O}_n, \hat{O}_m] = C_{nml}\hat{O}_l$. Here, C_{nml} are scalar coefficients, and the summation is performed over the repeated index. Suppose that the system Hamiltonian is a linear combination of $\{\hat{O}_n\}$, namely $\mathcal{H} = \sum_n a_n \hat{O}_n$ with a_n being real coefficients, the Liouvillian superoperator can thus be expressed as

$$\mathcal{L} = \begin{pmatrix} \sum_n a_n C_{n00} & \sum_n a_n C_{n10} & \cdots & \sum_n a_n C_{nd0} \\ \sum_n a_n C_{n01} & \sum_n a_n C_{n11} & \cdots & \sum_n a_n C_{nd1} \\ \vdots & \vdots & \ddots & \vdots \\ \sum_n a_n C_{n0d} & \sum_n a_n C_{n1d} & \cdots & \sum_n a_n C_{n dd} \end{pmatrix}. \quad (\text{S.25})$$

By solving the eigenvalue equation of the Liouvillian in this finite basis, namely $\mathcal{L}\hat{\Lambda}_k = \lambda_k \hat{\Lambda}_k$, the time-evolved interrogation operator is straightforwardly given by

$$\hat{O}(t) = \sum_{k=0}^d c_k e^{i\lambda_k t} \hat{\Lambda}_k \quad (\text{S.26})$$

where c_k are coefficients determined by the initial condition $\hat{O}(0) = \hat{O}$. It can be seen that if \mathcal{L} has

a *negative imaginary eigenvalue*, i.e. $\text{Im}(\lambda_k) < 0$ for certain k , the operator $\hat{O}(t)$ and subsequently the QFI by using Eq. (1) in the main text would exhibit an exponential blow-up in time. In contrast, for the scenario with $C_{nml} = C_{nlm}^*$, one can directly find that $\sum_n a_n C_{nml} = \sum_n a_n C_{nlm}^*$ for arbitrary values of $\{a_n\}$, which leads to the Hermiticity and thus a real spectrum of \mathcal{L} , such as the celebrated $su(2)$ algebra with $C_{nml} = i\varepsilon_{nml}$ and ε_{nml} denoting the Levi-Civita symbol. Consequently, the exponential blow-up of the QFI will be absent.

However, we remark that the above exponential blow-up usually holds only at short transient times, which highlights the significance of the main text focusing on the frequent infinite-dimensional scenario. The reason is that the Hamiltonian, resulting in that $\text{Im}(\lambda_k) < 0$, can only describe the exact system dynamics at very initial times. For example, the IHO effectively approximates to the famous quantum Rabi model or the LMG model by requiring the condition of low bosonic excitations [12], while the atomic three-mode spin-mixing realization of $SU(1, 1)$ interferometry is conditioned on the fact that a small fraction of population is transferred from the $m_f = 0$ to the $m_f = \pm 1$ hyperfine modes [13]; both conditions are satisfied only at a time scale much smaller than $\log(N)$. Below, we illustrate it using the inverted harmonic oscillator and the $SU(1, 1)$ interferometry.

In the first example of the IHO, the system dynamics is governed by an inverted harmonic trapping potential, with a Hamiltonian of the following form, $H = (P^2 - \lambda X^2)/2$ and $\lambda > 0$. The IHO Hamiltonian is one of the generators of area preserving transformations, which has been widely studied as a dilatation generator, a squeezing generator, or a Lorentz boost generator, with deep connections to quantum optics, quantum Hall systems and even quantum mechanics near event horizons of black holes [14]. Up to the second order of $\{X, P\}$, one can check that the Liouvillian superoperator can be solved in a simple closed basis of $\mathcal{X} = \{\mathbb{1}, X, P, K_0, K_+, K_-\}$ with $K_0 = (XP + PX)/4$ and $K_{\pm} = (P^2 \pm X^2)/4$. Explicitly,

$$\mathcal{L} = \begin{pmatrix} 0 & 0 & 0 & 0 & 0 & 0 \\ 0 & 0 & -i\lambda & 0 & 0 & 0 \\ 0 & -i & 0 & 0 & 0 & 0 \\ 0 & 0 & 0 & 0 & 0 & -(1-\lambda)i \\ 0 & 0 & 0 & 0 & 0 & -(1+\lambda)i \\ 0 & 0 & 0 & 0 & (1-\lambda)i & -(1+\lambda)i \end{pmatrix}. \quad (\text{S.27})$$

Both diagonal blocks of \mathcal{L} are non-Hermitian matrices, which respectively give rise to two negative imaginary eigenvalues, $-i\sqrt{\lambda}$ and $-2i\sqrt{\lambda}$. Consequently, the quadrature operators would evolve

as $X(t) \sim \exp(\sqrt{\lambda}t)$ and $K_+ \sim \exp(2\sqrt{\lambda}t)$. This further leads to an exponential form of the QFI growth, namely

$$F_Q[\rho(t), X] \sim \exp(2\sqrt{\lambda}t) \quad \text{and} \quad F_Q[\rho(t), K_+] \sim \exp(4\sqrt{\lambda}t). \quad (\text{S.28})$$

In quantum optics, we point out that the IHO is usually an approximate effective Hamiltonian for actual physical systems, such as the celebrated quantum Rabi model or Lipkin-Meshkov-Glick (LMG) model, by requiring the condition of low bosonic excitations in the system. More accurately, we illustrate this condition using the paradigmatic LMG example, the Hamiltonian of which reads,

$$\mathcal{H}_{\text{LMG}} = -\frac{\chi}{N} J_x^2 - \Omega J_z, \quad (\text{S.29})$$

where $\mathbf{J} = (J_x, J_y, J_z)$ represents the total spin operator of the system comprised of N spin-1/2 particles. When the system is initialized in a coherent spin state pointing along the positive z -axis, we can apply the Holstein-Primakoff transformation of the following form [15–17]

$$J_+ = J_x + iJ_y = \sqrt{N} \sqrt{1 - \frac{a^\dagger a}{N}} a, \quad (\text{S.30})$$

$$J_- = J_x - iJ_y = \sqrt{N} a^\dagger \sqrt{1 - \frac{a^\dagger a}{N}} \quad (\text{S.31})$$

$$J_z = \frac{N}{2} - a^\dagger a, \quad (\text{S.32})$$

where a (a^\dagger) represents the bosonic annihilation (creation) operator, obeying a standard commutation relation $[a, a^\dagger] = 1$. In the large N limit—that is, within the low bosonic excitation regime (i.e. the approximation $a^\dagger a/N \ll 1$ holds), Eq. (S.46) can be approximately simplified as

$$\mathcal{H}_{\text{LMG}} = \frac{\Omega}{2} P^2 + \frac{\Omega - \chi}{2} X^2, \quad \text{with} \quad X = \frac{a + a^\dagger}{\sqrt{2}}, \quad P = \frac{a - a^\dagger}{\sqrt{2}i}. \quad (\text{S.33})$$

By further setting that $\chi = 2\Omega > 0$, this is exactly an IHO with a maximally unstable trapping potential. The corresponding bosonic excitation of the system is given by

$$\langle a^\dagger a \rangle_t = \frac{1}{2} [\cosh(2\Omega t) - 1]. \quad (\text{S.34})$$

This result is logically valid only when $\langle a^\dagger a \rangle_t \ll N$. Consequently, one obtains that the evolution time should satisfy a condition that $t \ll \log N / 2\Omega$, in order to ensure the validity of the IHO approximation.

In the second example, we consider the $SU(1, 1)$ interferometry that is described by a closed $su(1, 1)$ algebra, namely

$$K_x = \frac{1}{2}(a_1^\dagger a_2^\dagger + a_1 a_2), \quad (\text{S.35})$$

$$K_y = -\frac{i}{2}(a_1^\dagger a_2^\dagger - a_1 a_2), \quad (\text{S.36})$$

$$K_z = \frac{1}{2}(a_1^\dagger a_1 + a_2 a_2^\dagger), \quad (\text{S.37})$$

where a_1 (a_1^\dagger) and a_2 (a_2^\dagger) describe two bosonic modes, satisfying commutation relations $[a_i, a_j^\dagger] = \delta_{ij}$. As a result, the commutation relations for the $su(1, 1)$ algebra are given by

$$[K_x, K_y] = -iK_z, \quad [K_y, K_z] = iK_x, \quad [K_z, K_x] = iK_y. \quad (\text{S.38})$$

In atomic systems, this $SU(1, 1)$ approach can be realized by exploiting a type of coherent spin-mixing dynamics in a spinor Bose-Einstein condensate. The spin-mixing dynamics describes a process of binary collisions, which can coherently transfer correlated pairs of trapped atoms from the $m_f = 0$ to the $m_f = \pm 1$ hyperfine modes with opposite magnetic moments. Explicitly, the associated many-body Hamiltonian in a dilute atomic cloud is given by [13]

$$\mathcal{H}_{\text{SMD}} = \frac{\chi}{N} (e^{-2i\phi} a_{+1}^\dagger a_{-1}^\dagger a_0 a_0 + e^{2i\phi} a_0^\dagger a_0^\dagger a_{+1} a_{-1}) + \frac{\chi}{N} \left(\hat{N}_0 - \frac{1}{2} \right) (\hat{N}_{+1} + \hat{N}_{-1}) + q(\hat{N}_{+1} + \hat{N}_{-1}), \quad (\text{S.39})$$

where N is the total atom number, χ is the coupling strength of spin-mixing interaction, q (ϕ) is the energy difference (relative phase) between the $m_f = 0$ and $m_f = \pm 1$ modes, a_i (a_i^\dagger) are bosonic annihilation (creation) operators for modes $i = m_f = 0, \pm 1$ obeying $[a_i, a_j^\dagger] = \delta_{ij}$, and $\hat{N}_i = a_i^\dagger a_i$ are the particle number operators. Experimentally, the spin-mixing process can be well controlled by microwave addressing. Theoretically, in the mean field limit—that is, the initial condensate contains a large number of particles in the $m_f = 0$ mode and the $m_f = 0$ mode operator can thus be replaced by a c -number, the spin-mixing operations belongs to the $SU(1, 1)$ group, namely

$$\mathcal{H}_{\text{SMD}} \approx 2\chi K_x + 2\tilde{q} K_z \quad (\text{S.40})$$

where we assume $\phi = 0$ and $\tilde{q} = q + \chi(1 - 1/2N)$. As a result, the Liouvillian governing the operator dynamics is given by

$$\mathcal{L} = \begin{bmatrix} 0 & -2i\tilde{q} & 0 \\ 2i\tilde{q} & 0 & -2i\chi \\ 0 & -2i\chi & 0 \end{bmatrix}. \quad (\text{S.41})$$

This matrix can have a negative imaginary eigenvalue, $-2i\sqrt{\chi^2 - \tilde{q}^2}$, when $\chi > \tilde{q}$. Particularly, if $\tilde{q} = 0$, one can obtain the operator dynamics as

$$K_z(t) = \sinh(2\chi t)K_y + \cosh(2\chi t)K_z, \quad (\text{S.42})$$

which implies generation of a Lorentz boost amplifying the population in the $m_f = \pm 1$ modes, namely

$$\langle \hat{N}_{+1} \rangle_t + \langle \hat{N}_{-1} \rangle_t = \cosh(2\chi t) - 1. \quad (\text{S.43})$$

We remark that this mean-field description is valid only when $\langle \hat{N}_{+1} \rangle_t + \langle \hat{N}_{-1} \rangle_t \ll N$, which requires that $t \ll \log N / 2\chi$.

V. Full quantum analysis of atomic $SU(1, 1)$ approach in Krylov space

In this section, we perform a full three-mode quantum analysis of the Hamiltonian in Eq. (S.39) for the atomic $SU(1, 1)$ interferometry. Noticing the symmetry of the system, we restrict to the Hilbert subspace spanned by Fock states $\{|N_{+1}, N_0, N_{-1}\rangle = |k, N - 2k, k\rangle\}$ with $0 \leq k \leq \lfloor N/2 \rfloor$. In this basis, the Hamiltonian when N is even can be expressed as

$$\mathcal{H}_{\text{SMD}} = \frac{\chi}{N} \begin{pmatrix} \alpha_0 & \beta_0 & 0 & 0 & \cdots & 0 \\ \beta_0 & \alpha_1 & \beta_1 & 0 & \cdots & 0 \\ 0 & \beta_1 & \alpha_2 & \beta_2 & \cdots & 0 \\ 0 & 0 & \beta_2 & \alpha_3 & \ddots & 0 \\ \vdots & \vdots & \vdots & \ddots & \ddots & \beta_{\frac{N}{2}-1} \\ 0 & 0 & 0 & 0 & \beta_{\frac{N}{2}-1} & \alpha_{\frac{N}{2}} \end{pmatrix} + q \begin{pmatrix} 0 & 0 & 0 & 0 & \cdots & 0 \\ 0 & 2 & 0 & 0 & \cdots & 0 \\ 0 & 0 & 4 & 0 & \cdots & 0 \\ 0 & 0 & 0 & 6 & \ddots & 0 \\ \vdots & \vdots & \vdots & \ddots & \ddots & 0 \\ 0 & 0 & 0 & 0 & 0 & N \end{pmatrix}, \quad (\text{S.44})$$

where $\alpha_k = 2k(N - 2k - 1/2)$ and $\beta_k = (k + 1)\sqrt{(N - 2k)(N - 2k - 1)}$. We consider the conventional interrogation operator $\hat{\mathcal{O}} = (N_{+1} + N_{-1})/2$, which is given by the following matrix,

$$\hat{\mathcal{O}} = \begin{pmatrix} 0 & 0 & 0 & 0 & \cdots & 0 \\ 0 & 1 & 0 & 0 & \cdots & 0 \\ 0 & 0 & 2 & 0 & \cdots & 0 \\ 0 & 0 & 0 & 3 & \ddots & 0 \\ \vdots & \vdots & \vdots & \ddots & \ddots & 0 \\ 0 & 0 & 0 & 0 & 0 & \frac{N}{2} \end{pmatrix}, \quad (\text{S.45})$$

the Lanczos coefficients can be numerically determined.

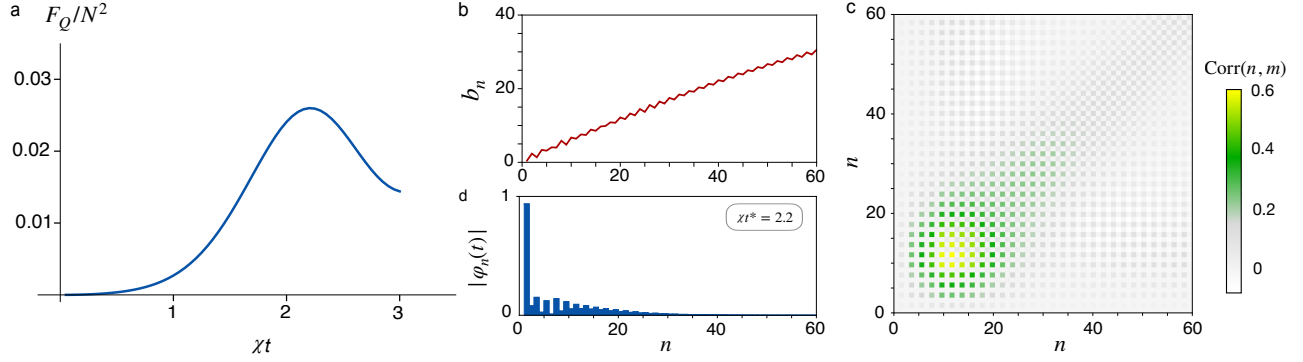


FIG. S7. **QFI dynamics and its behavior in Krylov space by $SU(1,1)$ approach.** (a) The QFI achieves its first local maximum around $\chi t^* = 2.2$. (b) The Lanczos coefficients $\{b_n\}$ show a linear increase up to the order of $n_L \simeq N$. (c) The correlation landscape $\text{Corr}(n, m)$ is dominated by its diagonal stripe and exhibit a local maximum around $(n^*, n^*) \approx (15, 15)$. (d) The fact that $n_L \gtrsim 4n^*$ leads to that the operator wavefunction at $t^* \approx 2.2/\chi$ when the QFI is approximately optimized, is fully covered by the linearly increased region of the Lanczos coefficients, implying that the first local maximum of the QFI can be achieved exponentially fast. We choose the particle number as $N = 60$ and the system parameters as $\chi = 1$ and $q = -1$.

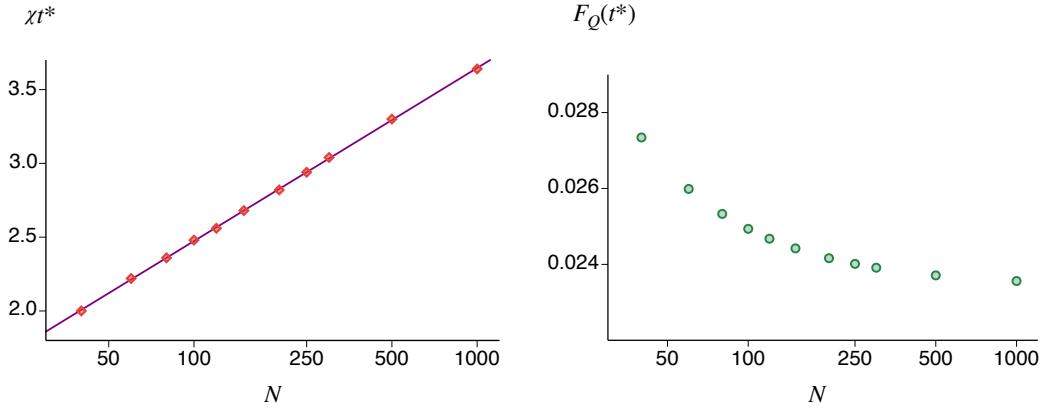


FIG. S8. **Exponentially fast entanglement generation by $SU(1,1)$ approach.** (a) The evolution time t^* at which the QFI achieves its optimum shows a logarithmic relation with the particle number of the system, i.e. $\chi t^* \approx 0.51 \log N + 0.13$. (b) The maximal QFI at the time t^* approximately saturates to $F_Q(t^*) \approx 0.024N^2$ in the large- N limit. We set the system parameters as $\chi = 1$ and $q = -1$.

We consider the regime where the Liouvillian in Eq. (S.40) has a negative imaginary eigenvalue by setting $\chi = 1$ and $q = -1$. The corresponding numerical results in Krylov space are shown in

Fig. S7. The Lanczos coefficients show a linear increase asymptotics, and the linear region fully covers the dominant diagonal part of the correlation landscape, which indicates an exponentially fast approaching of the first local maximum of the QFI (approximately at the time $\chi t^* = 2.2$). However, one can also see that the main population of $\varphi_n(t^*)$ still stays in the first few sites, which however contribute a very small QFI. Consequently, the maximal QFI can not significantly break the standard quantum limit—that is $F_Q(t^*) \simeq \epsilon N^2$ with $\epsilon \approx 0.024 \ll 1$ (see Fig. S8).

VI. Effect of physical imperfections and decoherence

Apart from the fundamental interest in quantum theory, creating many-particle entangled states in an exponentially fast speed is also of great importance for developing cutting-edge quantum enhanced technologies. Therefore, the physical implementation in presence of imperfections and

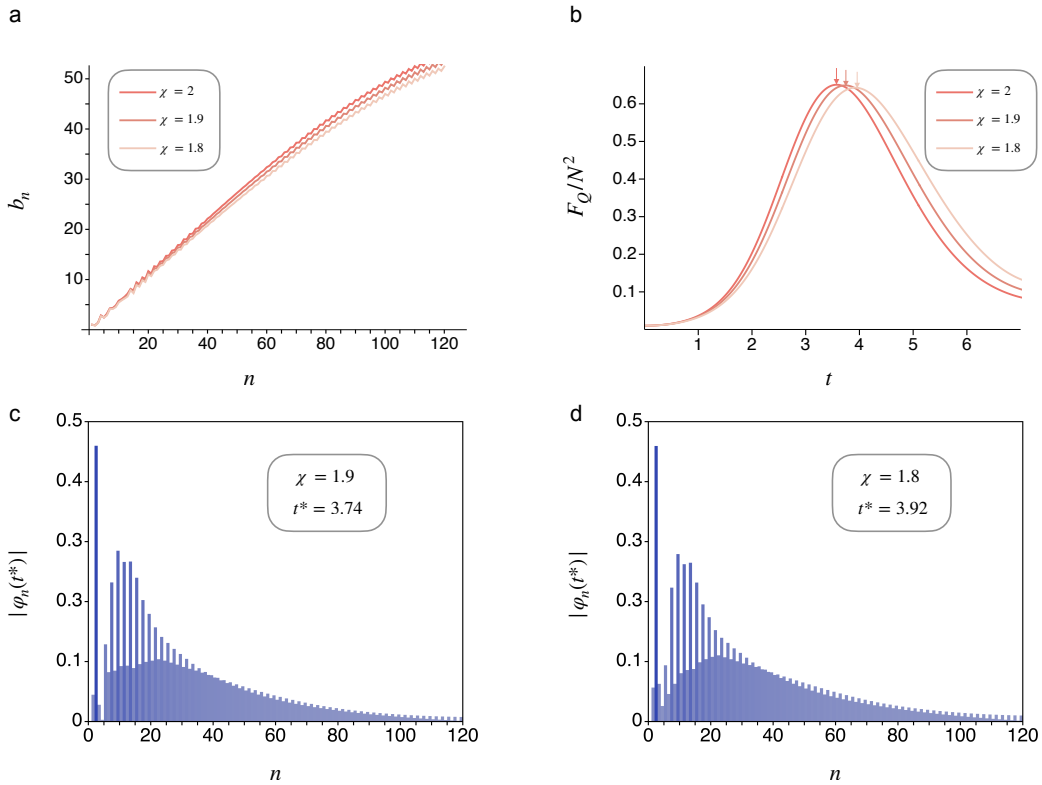


FIG. S9. **Effect of physical imperfections of the Hamiltonian parameter in LMG model.** (a-b) The Lanczos coefficients and the QFI dynamics for $\Omega = 1$ and different values of χ . (c-d) The operator wavefunctions when the QFI achieves its maximum are almost completely covered by the linear region of the Lanczos coefficients for both $\chi = 1.9$ and $\chi = 1.8$. Therefore, the exponentially fast generation of global entanglement is robust against the variation of the parameter χ . Here the system size is set as $N = 100$.

decoherence in explicit quantum platforms should be carefully considered. In this section, we briefly discuss the effect of physical imperfections in implementing the entanglement generating Hamiltonian and decoherence due to interactions with the environment.

Firstly, we study the effect of physical imperfections. Considering the two examples investigated in our main text, the saddle-point dominated scrambling dynamics in the LMG model and the chaotic quantum dynamics in FP model occurs for a wide range of parameter region (i.e. $0 < \Omega < \chi/2$ and $-1 < c < 1$ respectively). This fact implies that the exponentially fast behavior of entanglement generation can be robust to variations of the system parameters. As an illustrative example, we investigate the LMG model for different values of the interaction parameter χ in Fig. S9, which demonstrates the robustness to physical imperfections of the system parameter. In

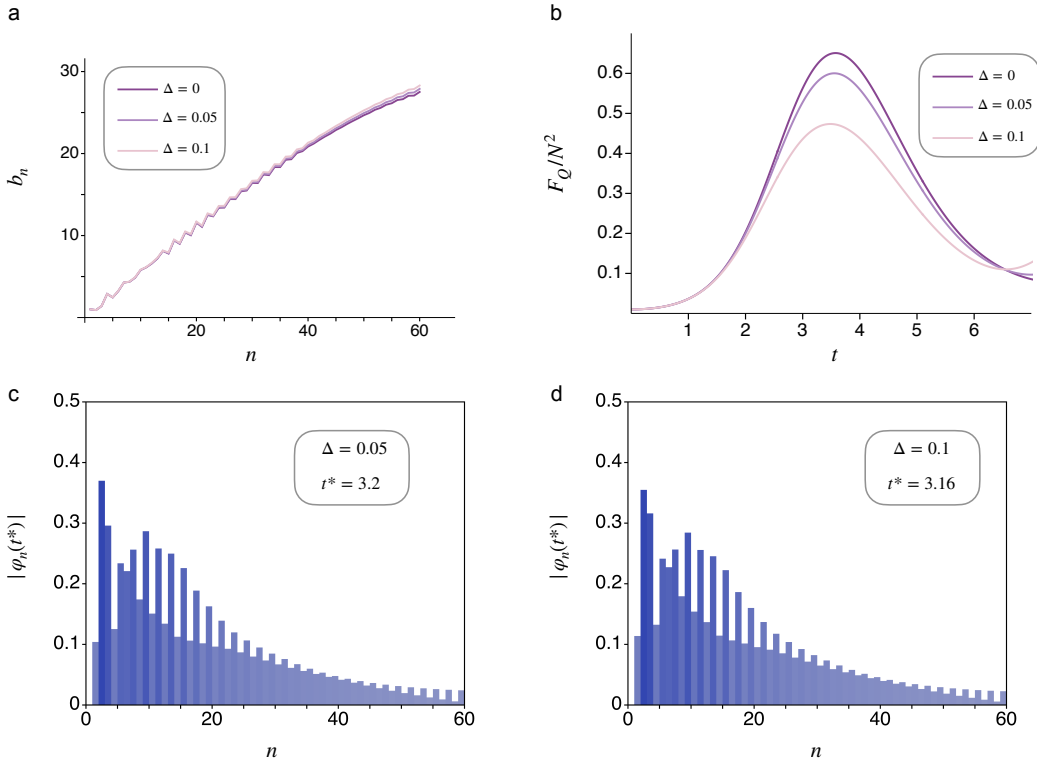


FIG. S10. **Effect of physical imperfections of the unwanted transverse field in LMG model.** (a-b) The Lanczos coefficients and the QFI dynamics for $\chi = 2\Omega = 2$ and different values of Δ in Eq. (S.46). (c-d) The operator wavefunctions when the QFI achieves its maximum are approximately covered by the linear region of the Lanczos coefficients for both $\Delta = 0.05$ and $\Delta = 0.1$. Therefore, the exponentially fast generation of multipartite entanglement is robust against a certain level of imperfections of the transverse field. Here the system size is set as $N = 50$.

addition, we also consider the effect of other unwanted terms when engineering the Hamiltonian, for instance, small transverse field of other directions in the LMG model,

$$\mathcal{H}'_{\text{LMG}} = -\frac{\chi}{N} J_x^2 - \Omega J_z + \Delta J_x. \quad (\text{S.46})$$

Our numerical results in Fig. S10 shows that the linear asymptotics of the Lanczos coefficients and the corresponding exponentially fast entangling dynamics can sustain with such a type of physical imperfections as well.

Secondly, we consider the effect of decoherence due to the inevitable interaction with environment. It should be pointed out that our framework based on Eq. (1) of the main text is applicable to QFI dynamics in closed systems. Currently, it is still very elusive to link QFI dynamics to the operator evolution in open quantum systems. Moreover, the Krylov approach to characterize operator delocalization, to the best of our knowledge, also merely considers the unitary dynamics governed by the system Hamiltonian, except for a very recent extension (see Ref. [18]). However, the extension assumes a Lindblad evolution of the operator to include the decoherence. Such an assumption of operator evolution cannot be simply exploited in Eq. (1) of our main text to capture the QFI dynamics. Therefore, the question how the entanglement generation speed is related to the Lanczos coefficients remains a challenging but interesting direction in the future research. Here,

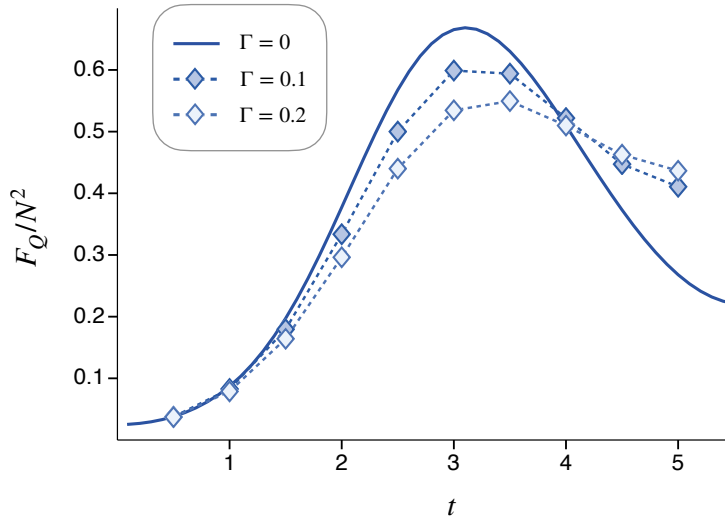


FIG. S11. **Effect of decoherence in LMG model.** We numerically derive the QFI dynamics $F_Q[\rho(t), J_x]$ for different strengths of the dephasing noises. It can be seen that the optimal time when the QFI achieves its maximum are almost the same, indicating that the exponentially fast entangling dynamics is robust to a certain level of dephasing effect. Here the system parameter is set as $\chi = 2\Omega = 2$ and $N = 40$.

we briefly study the decoherence effect by considering the LMG model through direct numerical simulation. As a simple example, we include the following dephasing noise,

$$\partial_t \rho = \mathcal{L}\rho = -i[\mathcal{H}_{\text{LMG}}, \rho] + \Gamma \left(J_z \rho J_z - \frac{1}{2} \{J_z^2, \rho\} \right) \quad (\text{S.47})$$

We solve this equation by vectorize the density operator of the system, i.e. $\rho \rightarrow |\rho\rangle\rangle$. We use the convention of the row-major vectorization, which leads the following form of the Lindblad operator governing the system dynamics

$$\mathcal{L} = -i(\mathcal{H}_{\text{LMG}} \otimes \mathbb{1} - \mathbb{1} \otimes \mathcal{H}_{\text{LMG}}^T) + \Gamma \left[J_z \otimes J_z^* - \frac{1}{2} (J_z^2 \otimes \mathbb{1} + \mathbb{1} \otimes J_z^2) \right]. \quad (\text{S.48})$$

Subsequently, the time-evolved density operator is given by

$$|\rho(t)\rangle\rangle = e^{\mathcal{L}t} |\rho(0)\rangle\rangle. \quad (\text{S.49})$$

Based on the density operator, we calculate the QFI using the following formula,

$$F_Q[\rho(t), \hat{O}] = 2\gamma \text{tr}([\hat{O}, \sqrt{\rho(t)}]^\dagger [\hat{O}, \sqrt{\rho(t)}]). \quad (\text{S.50})$$

As one sees in Fig. S11, our straightforward numerical simulation demonstrates that the exponentially fast entanglement generation can sustain to a certain level of environmental noise.

VII. Optimal interrogation operator for the entangling dynamics

As one can see in Eq. (1) of the main text, the value of the QFI has close relation with the interrogation operator. For a generic multipartite interacting system, however, there is still no simple universal principles that are capable of analytically determining the optimal interrogation operator, to our best knowledge. After identifying a multipartite interacting system that enables exponentially fast generation of an entangled state ρ , the most straightforward way to obtain the optimal interrogation operator is optimizing the QFI value by exact numerical calculation. Given a finite-dimensional optimization set of the interrogation operator, for example, $\{O_1, O_2, \dots, O_q\}$, we can expand the interrogation operator as $O = \sum_{\mu=1}^q \lambda_\mu O_\mu$ with $\sum_{\mu=1}^q |\lambda_\mu|^2 = 1$. Then the QFI can be re-expressed as

$$F_Q[\rho, O] = \sum_{\mu\nu} 2\gamma \lambda_\mu^* \lambda_\nu \text{tr}([O_\mu, \sqrt{\rho}]^\dagger [O_\nu, \sqrt{\rho}]). \quad (\text{S.51})$$

For pure state $\rho = |\Psi\rangle\langle\Psi|$, it further simplifies to

$$F_Q = \boldsymbol{\lambda}^T \cdot \mathcal{F} \cdot \boldsymbol{\lambda}, \quad (\text{S.52})$$

where the vector is defined as $\boldsymbol{\lambda} = (\lambda_1, \dots, \lambda_q)^T$, and the matrix \mathcal{F} coincidentally corresponds to the quantum Fisher information matrix (QFIM) that characterizes the multi-parameter dependent state $e^{-i\sum_\mu \theta_\mu O_\mu} |\Psi\rangle$ [19]. The explicit form of QFIM component is given by

$$\mathcal{F}_{\mu\nu} = 2\langle O_\mu O_\nu + O_\nu O_\mu \rangle - 4\langle O_\mu \rangle \langle O_\nu \rangle. \quad (\text{S.53})$$

By diagonalizing the QFIM, i.e. $F_Q = \boldsymbol{\lambda}^\dagger U^\dagger \mathcal{F}_\Lambda U \boldsymbol{\lambda}$, one can see that the largest QFI that can be achieved by the largest eigenvalue of the QFIM and the corresponding optimal interrogation operator is determined by the related eigenvector. More specifically, if $\mathcal{F}\boldsymbol{\lambda}^{(m)} = F^{(\max)}\boldsymbol{\lambda}^{(m)}$, the optimal QFI is then given by $F^{(\max)}$ and the optimal interrogation operator is

$$O^{(m)} = \sum_{\mu=1}^q \lambda_\mu^{(m)} O_\mu. \quad (\text{S.54})$$

Taking the LMG model investigated in the main text as example, $|\Psi\rangle = e^{-i\mathcal{H}_{\text{LMG}}t^*} |\uparrow\uparrow \dots \uparrow\rangle$ with $t^* \approx 3.8$, the QFIM is given by

$$\mathcal{F} \approx \begin{bmatrix} 0.647 & 0.001 & 0 \\ 0.001 & 0.132 & 0 \\ 0 & 0 & 0.105 \end{bmatrix}. \quad (\text{S.55})$$

Therefore, the optimal interrogation operator is approximately given by $O^{(m)} \approx J_x$, that is exactly what we considered in the main text.

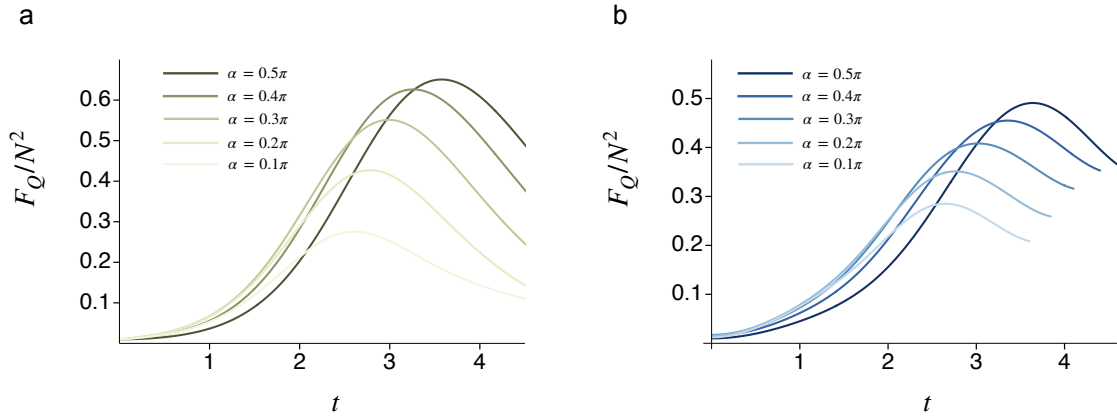


FIG. S12. **Correlated behaviors between the exact and approximated QFI in LMG model.** (a) The exact QFI is directly calculated for the interrogation operators $J_\alpha = \sin(\alpha)J_x + \cos(\alpha)J_y$ and achieves the maximal value at $\alpha \approx 0.5\pi$, i.e. $J_\alpha \approx J_x$. (b) The QFI variant, $\mathcal{F}_Q = 4\sum_n \bar{f}_n \varphi_n^2(t)$, defined by Eq. (10) in the main text, shows strongly correlated behaviors with the exact QFI dynamics. Here, the system size is set as $N = 100$ and the relevant parameters are $\chi = 2\Omega = 2$ and $w = 10$.

We also point out that the correlated behaviors between the QFI variant defined by Eq. (10) in the main text and the exact QFI might also help us to choose the interrogation operator by looking at the maximal values that the QFI variant can achieve. We illustrate this result in detail by the LMG model, as shown in Fig. S12.

* jianmingcai@hust.edu.cn

- [1] P. Caputa, J. M. Magan, and D. Patramanis, Geometry of Krylov complexity, *Phys. Rev. Res.* **4**, 013041 (2022).
- [2] D. E. Parker, X. Cao, A. Avdoshkin, T. Scaffidi, and E. Altman, A universal operator growth hypothesis, *Phys. Rev. X* **9**, 041017 (2019).
- [3] L. Pezzè, A. Smerzi, M. K. Oberthaler, R. Schmied, and P. Treutlein, Quantum metrology with non-classical states of atomic ensembles, *Rev. Mod. Phys.* **90**, 035005 (2018).
- [4] S. Pang and T. A. Brun, Quantum metrology for a general Hamiltonian parameter, *Phys. Rev. A* **90**, 022117 (2014).
- [5] Y. Chu, S. Zhang, B. Yu, and J. Cai, Dynamic framework for criticality-enhanced quantum sensing, *Phys. Rev. Lett.* **126**, 010502 (2021).
- [6] C. Hotter, H. Ritsch, and K. Gietka, Combining critical and quantum metrology, *Phys. Rev. Lett.* **132**, 060801 (2024).
- [7] K. Gietka, L. Ruks, and T. Busch, Understanding and improving critical metrology. Quenching super-radiant light-matter systems beyond the critical point, *Quantum* **6**, 700 (2022).
- [8] Z. Li, S. Colombo, C. Shu, G. Velez, S. Pilatowsky-Cameo, R. Schmied, S. Choi, M. Lukin, E. Pedrozo-Peñañiel, and V. Vuletić, Improving metrology with quantum scrambling, *Science* **380**, 1381 (2023).
- [9] B. Yurke, S. L. McCall, and J. R. Klauder, SU(2) and SU(1,1) interferometers, *Phys. Rev. A* **33**, 4033 (1986).
- [10] C. Gross, T. Zibold, E. Nicklas, J. Estève, and M. K. Oberthaler, Nonlinear atom interferometer surpasses classical precision limit, *Nature* **464**, 1165 (2010).
- [11] Q. Liu, L.-N. Wu, J.-H. Cao, T.-W. Mao, X.-W. Li, S.-F. Guo, M. K. Tey, and L. You, Nonlinear interferometry beyond classical limit enabled by cyclic dynamics, *Nat. Phys.* **18**, 167 (2022).
- [12] M.-J. Hwang, R. Puebla, and M. B. Plenio, Quantum phase transition and universal dynamics in the

- Rabi model, *Phys. Rev. Lett.* **115**, 180404 (2015).
- [13] M. Gabbriellini, L. Pezzè, and A. Smerzi, Spin-mixing interferometry with Bose-Einstein condensates, *Phys. Rev. Lett.* **115**, 163002 (2015).
- [14] V. Subramanyan, S. S. Hegde, S. Vishveshwara, and B. Bradlyn, Physics of the inverted harmonic oscillator: From the lowest Landau level to event horizons, *Ann. Phys.* **435**, 168470 (2021).
- [15] J. Vidal, G. Palacios, and C. Aslangul, Entanglement dynamics in the lipkin-meshkov-glick model, *Phys. Rev. A* **70**, 062304 (2004).
- [16] S. Dusuel and J. Vidal, Finite-size scaling exponents of the lipkin-meshkov-glick model, *Phys. Rev. Lett.* **93**, 237204 (2004).
- [17] S. Dusuel and J. Vidal, Continuous unitary transformations and finite-size scaling exponents in the lipkin-meshkov-glick model, *Phys. Rev. B* **71**, 224420 (2005).
- [18] C. Liu, H. Tang, and H. Zhai, Krylov complexity in open quantum systems, *Phys. Rev. Res.* **5**, 033085 (2023).
- [19] J. T. Reilly, J. D. Wilson, S. B. Jäger, C. Wilson, and M. J. Holland, Optimal generators for quantum sensing, *Phys. Rev. Lett.* **131**, 150802 (2023).